Searching for non-gravitational signatures of Dark Matter in the Galactic Center

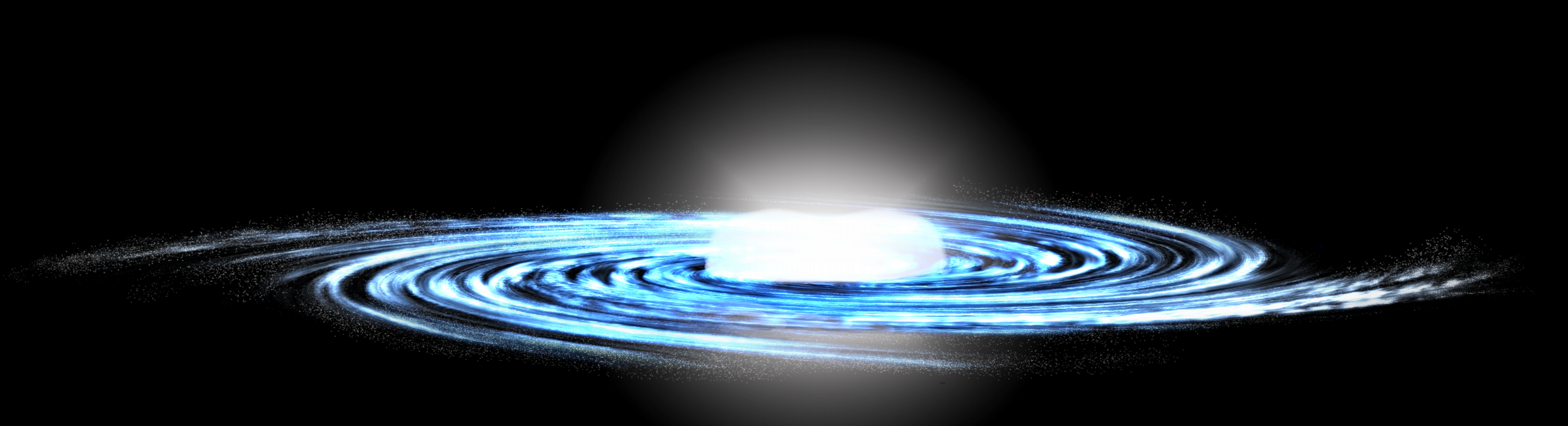

O. Macias, C. Gordon, R. Crocker, S. Horiuchi, D. Paterson, B. Coleman and M. Pohl

[Nat. Astr. 2 (2018) no.5, 387-392]

Kavli Institute for the Physics and Mathematics of the Universe (WPI)

Nov. 9, (2018)

Evidence for the Existence of Dark Matter

1) Rotational Curves

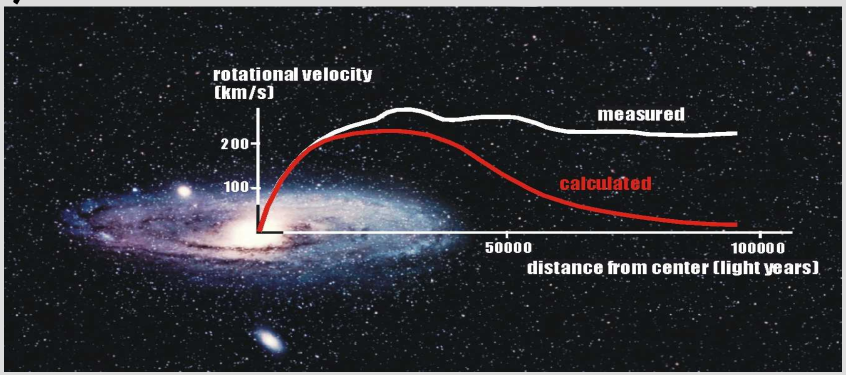

Image Credit:http://cdms.phy.queensu.ca/Public_Docs/DM_Intro.html

2) Bullet Cluster

Image Credit:M.Markevitch et al./ D.Clowe et al.; D.Clowe et al.

3) CMB

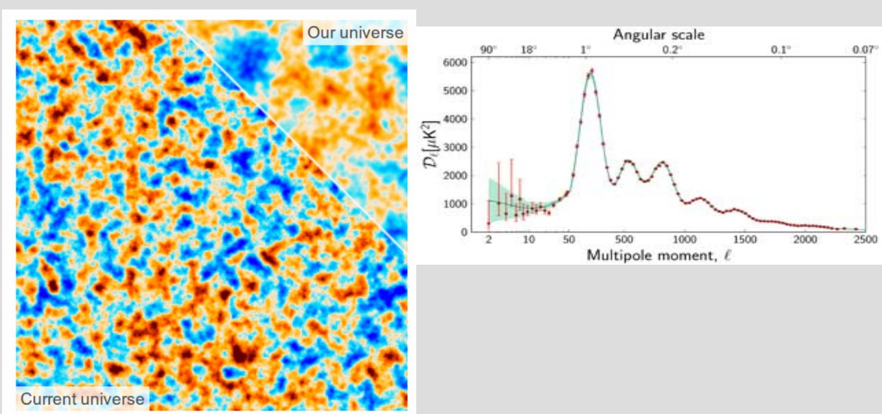

Image Credit: by Amanda Yoho on the Planck CMB http://strudel.org.uk/planck/# and Planck Collaboration.

4) Large Scale Structure

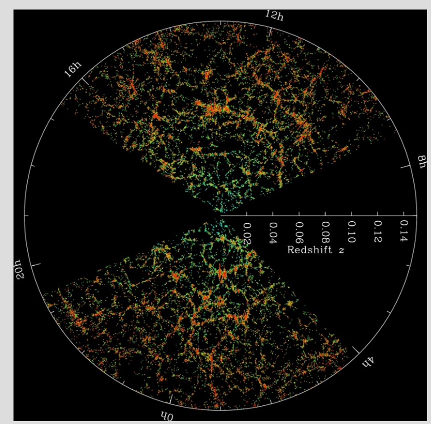

Image Credit:"Sloan Digital Sky Survey 1.25 Declination Slice 2013 Data" by M. Blanton and Sloan coll.

Dark Matter candidates and the WIMP miracle

- Dark Matter candidates must be non-baryonic, cold or warm and must be long lived.
- There are many dark matter candidates, but particles with mass ~ 100 GeV have a privileged position.
- Particle physics independently predicts particles with the right relic density to be dark matter.

HEPPAP/AAAC DMSAG Subpanel (2007)

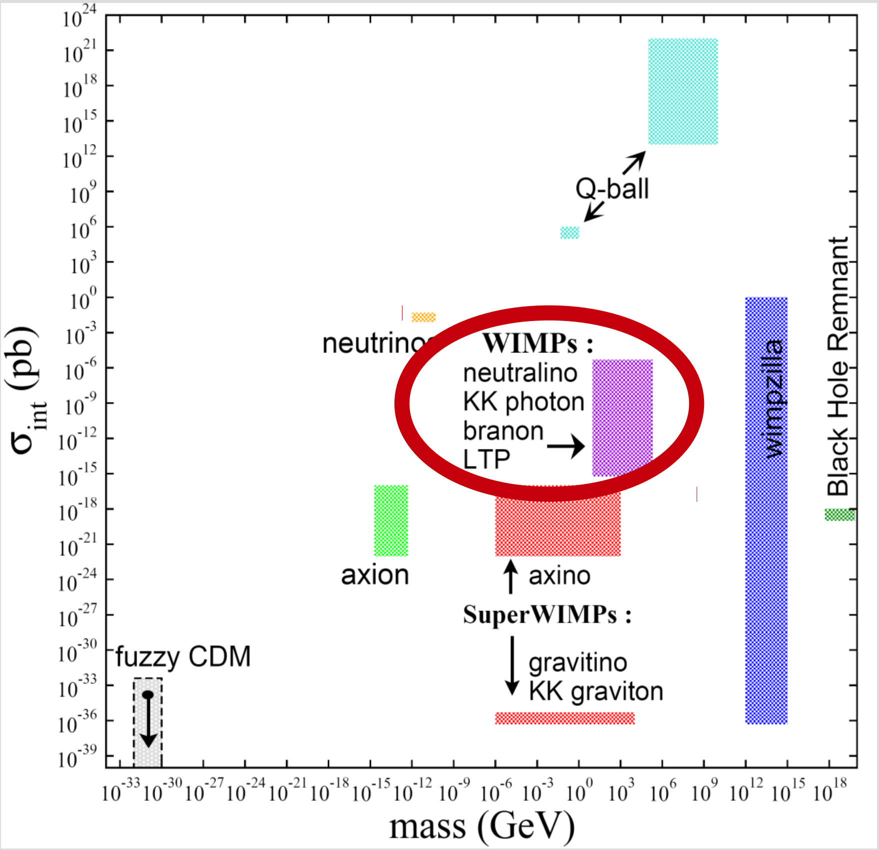

Fermi Gamma-ray Space Telescope (2008 - present)

- Fermi-LAT is a space based gamma-ray detector with an effective energy range of 20 MeV-500 GeV.
- Effective Area $\sim 0.8\,\mathrm{m}^2$
- Field of view ~2.4 sr
- Energy resolution ~10%
- Angular resolution is energy dependent

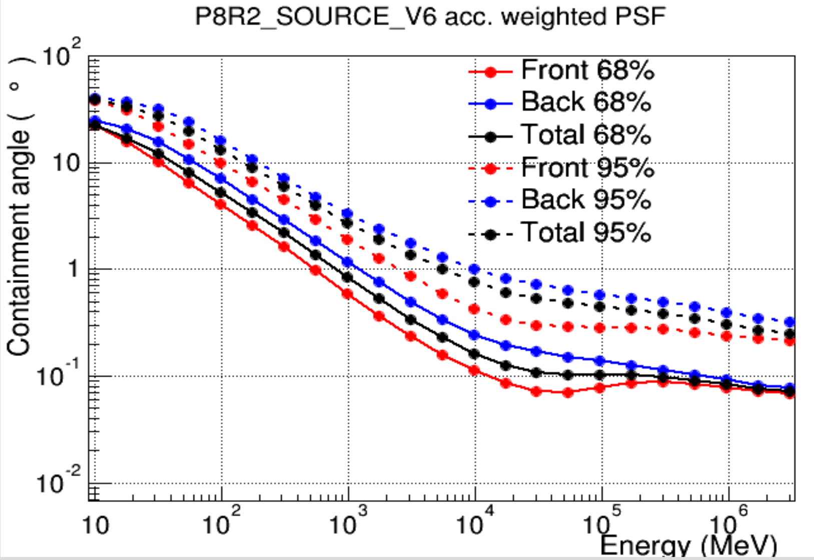

Image Credit: https://www.slac.stanford.edu/exp/glast/groups/canda/lat_Performance.htm

Where to look for dark matter emission?

Galactic Halo:
- ✓ Large Statistics
- ✓ Uncertain Backgroud

Galactic Center:
- ✓ Large Statistics
- ✓ Uncertain Background

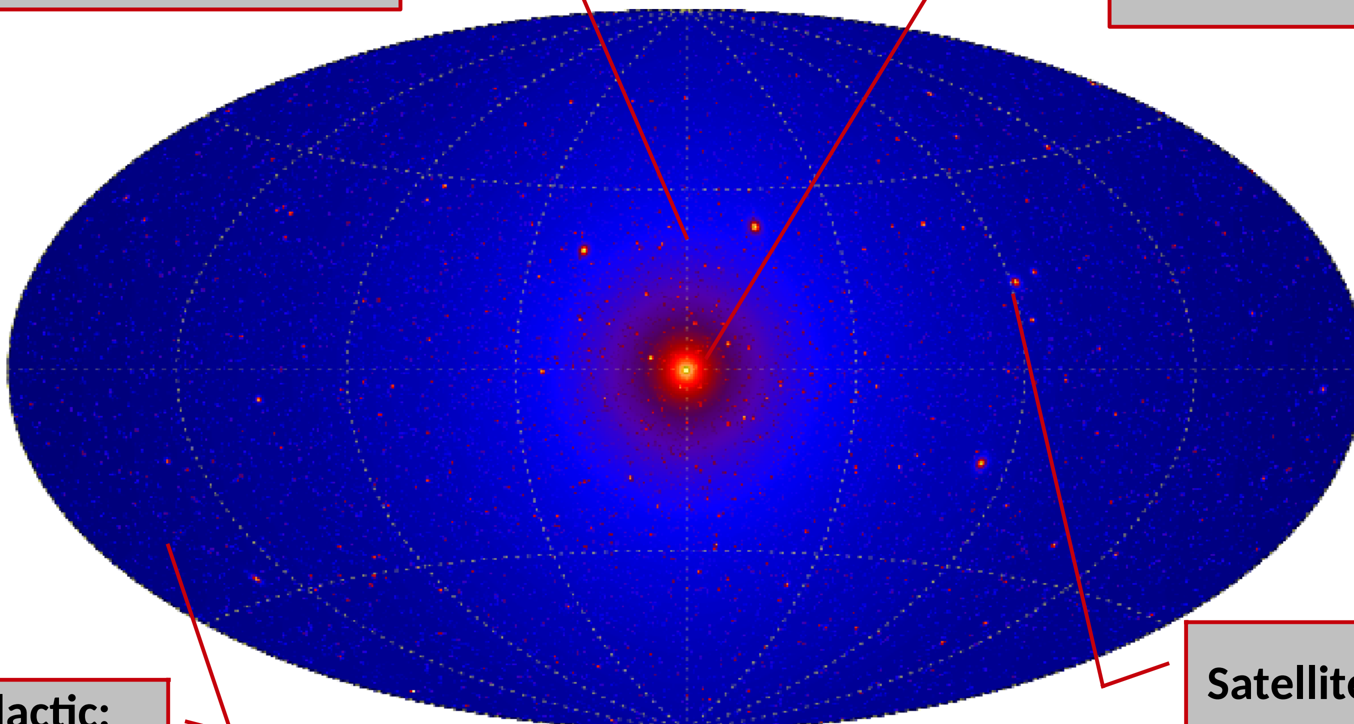

Extragalactic:
- ✓ Isotropic
- ✓ Clusters
- ✓ Uncertain background

All sky map of gamma-rays from DM annihilation (Via Lactea II simulation), arXiv:0908.0195

Satellite Galaxies:
- ✓ Low statistics
- ✓ Clean background
- ✓ Uncertain DM distribution

The center of our Galaxy is one of the most interesting places to look for DM annihilations

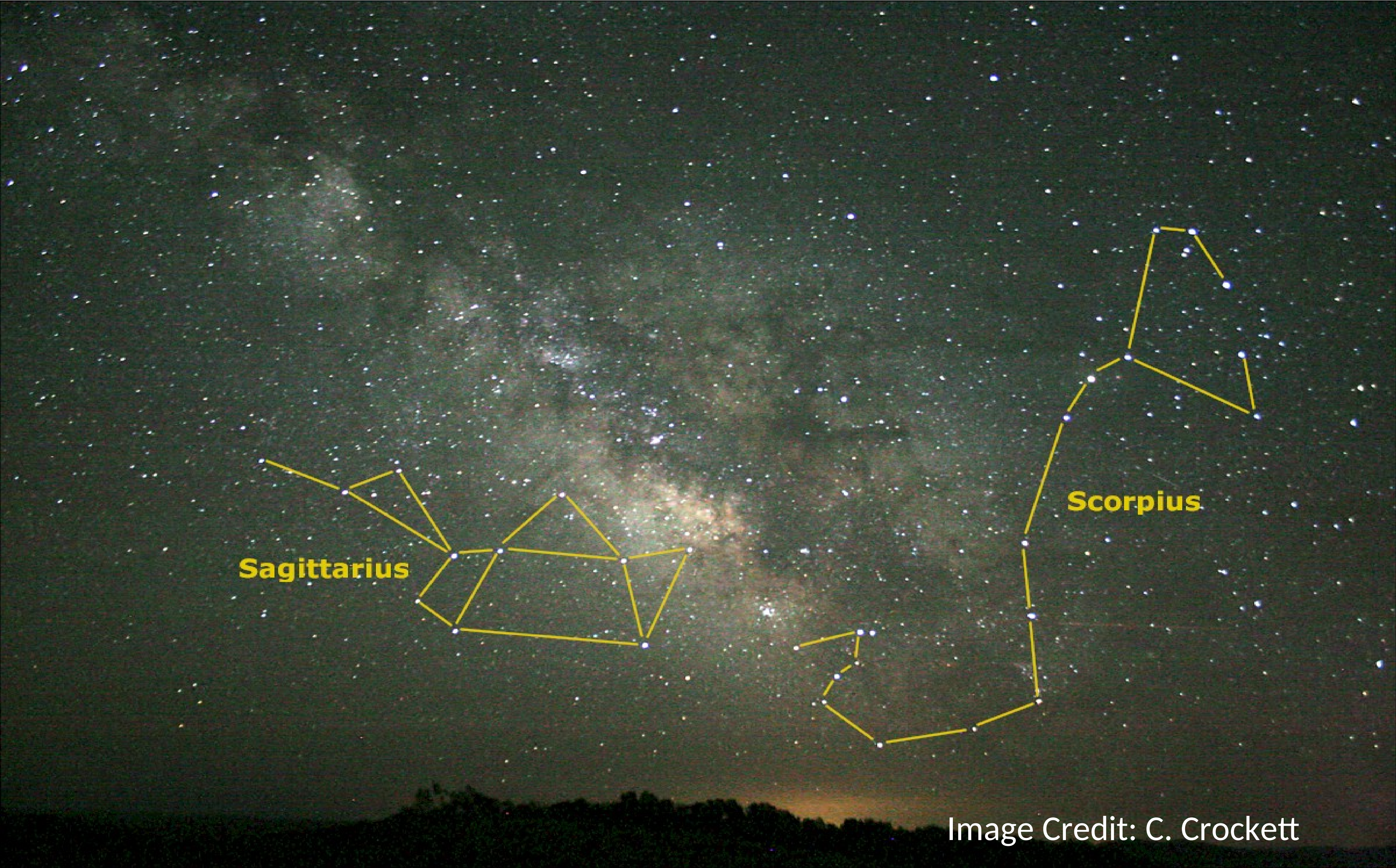

Image Credit: C. Crockett

Many studies have found an excess of gamma-rays at the Galactic Center

- **Spatial morphology**

$$\boxed{\propto r^{-2.4}}$$

- **Energy Spectrum**

$$\boxed{\propto E^{-\Gamma}\exp(-E/E_{\mathrm{cut}})}$$

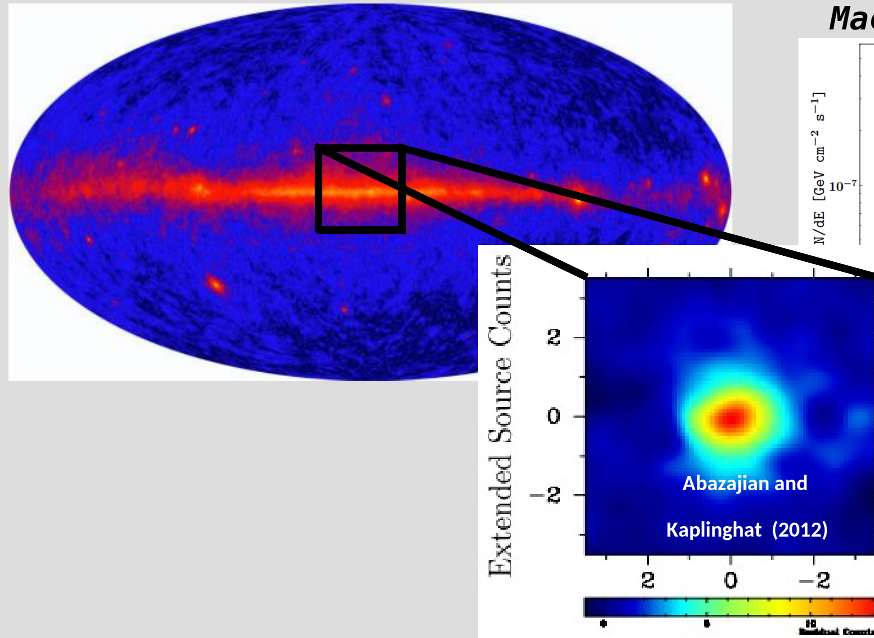

Gordon and Macias (2013)

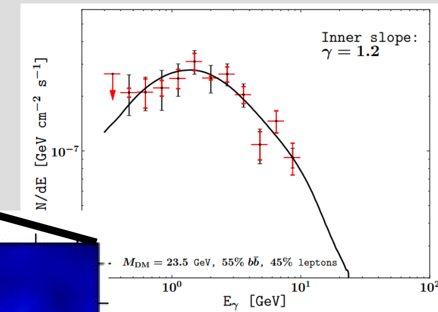

Many studies have found an excess of gamma-rays at the Galactic Center

- **Spatial morphology**

$$\boxed{\propto r^{-2.4}}$$

- **Energy Spectrum**

$$\boxed{\propto E^{-\Gamma}\exp(-E/E_{\rm cut})}$$

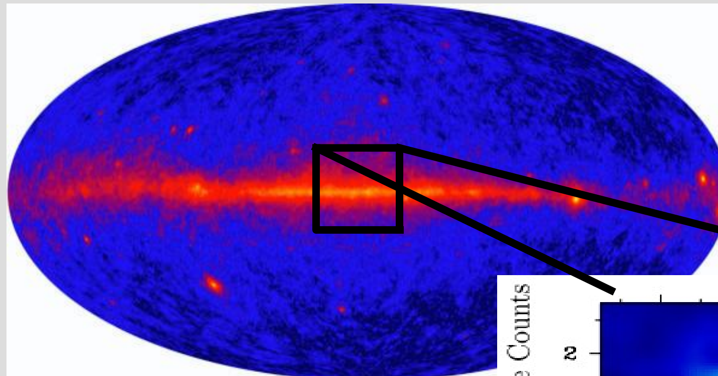

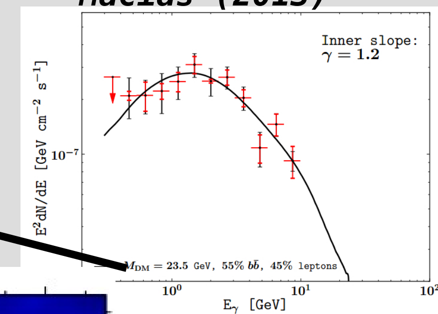

Gordon and Macias (2013)

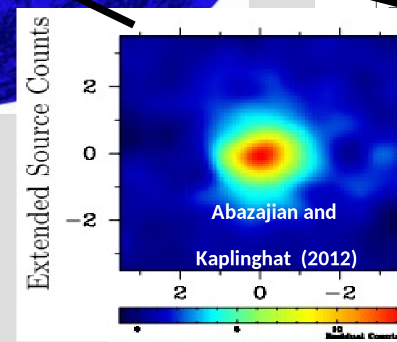

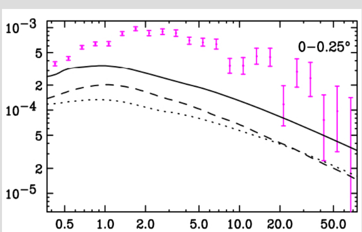

Goodenough and Hooper (2009)

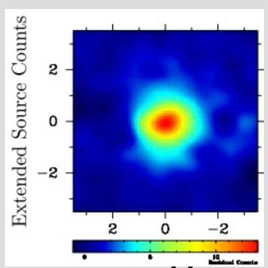

Abazajian and Kaplinghat (2012)

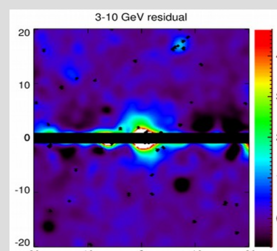

Daylan et al.(2016)

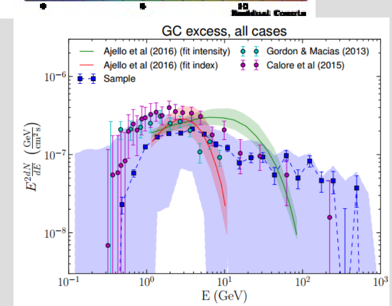

Ackermann et al.(2017)

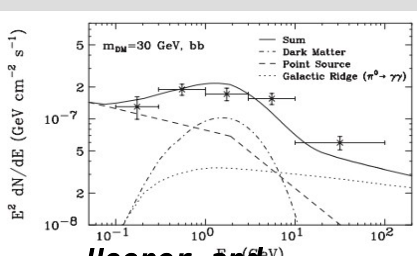

Hooper and Linden (2011)

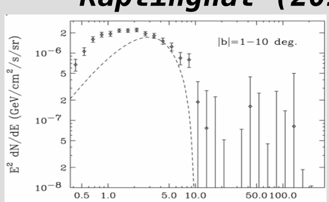

Hooper and Slatyer (2013)

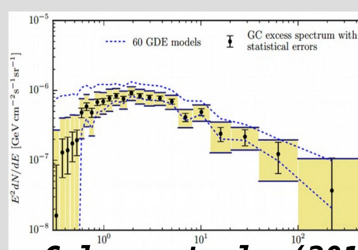

Calore et al. (2015)

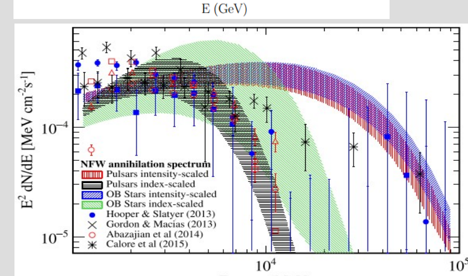

Ajello et al. (2016)

The Galactic diffuse emission is the most important component at the Galactic Center

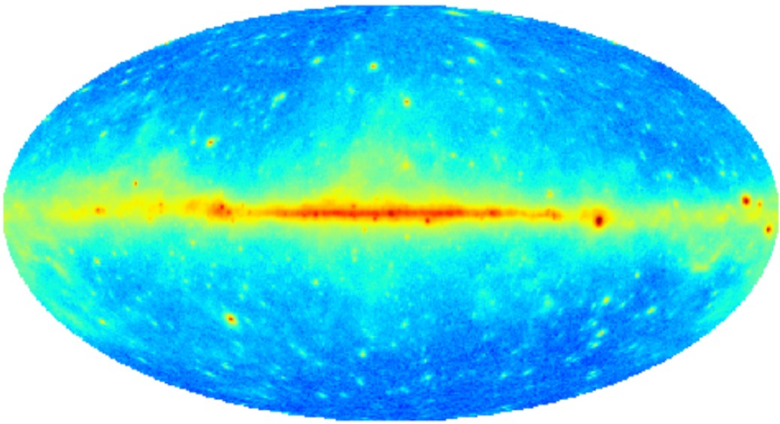

Data

=

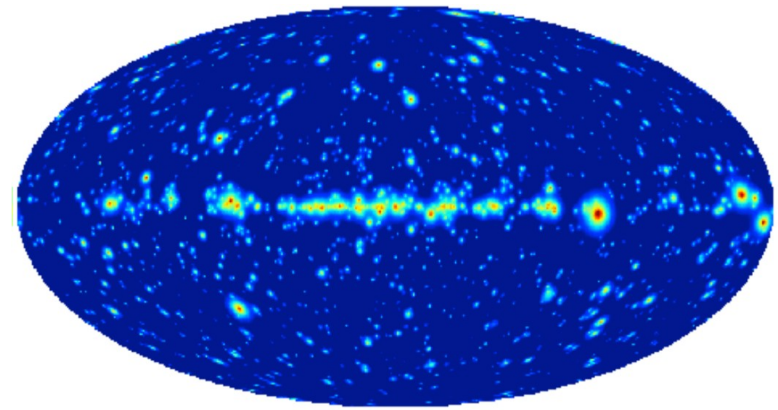

Point sources

+

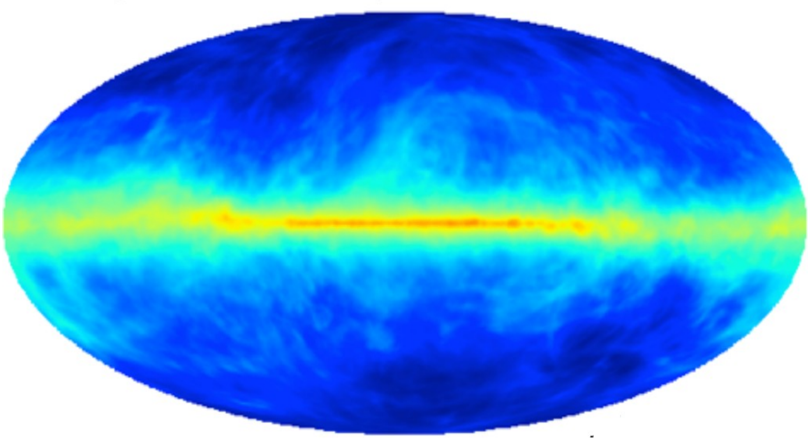

Galactic Diffuse

+

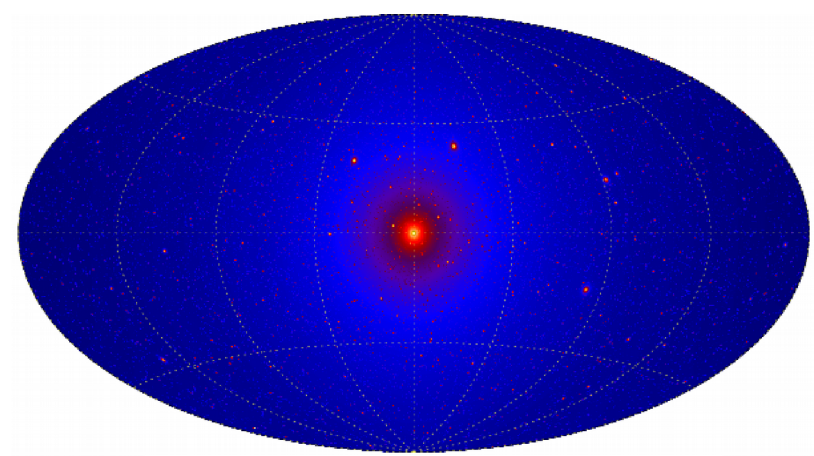

Dark Matter?

Galactic diffuse components

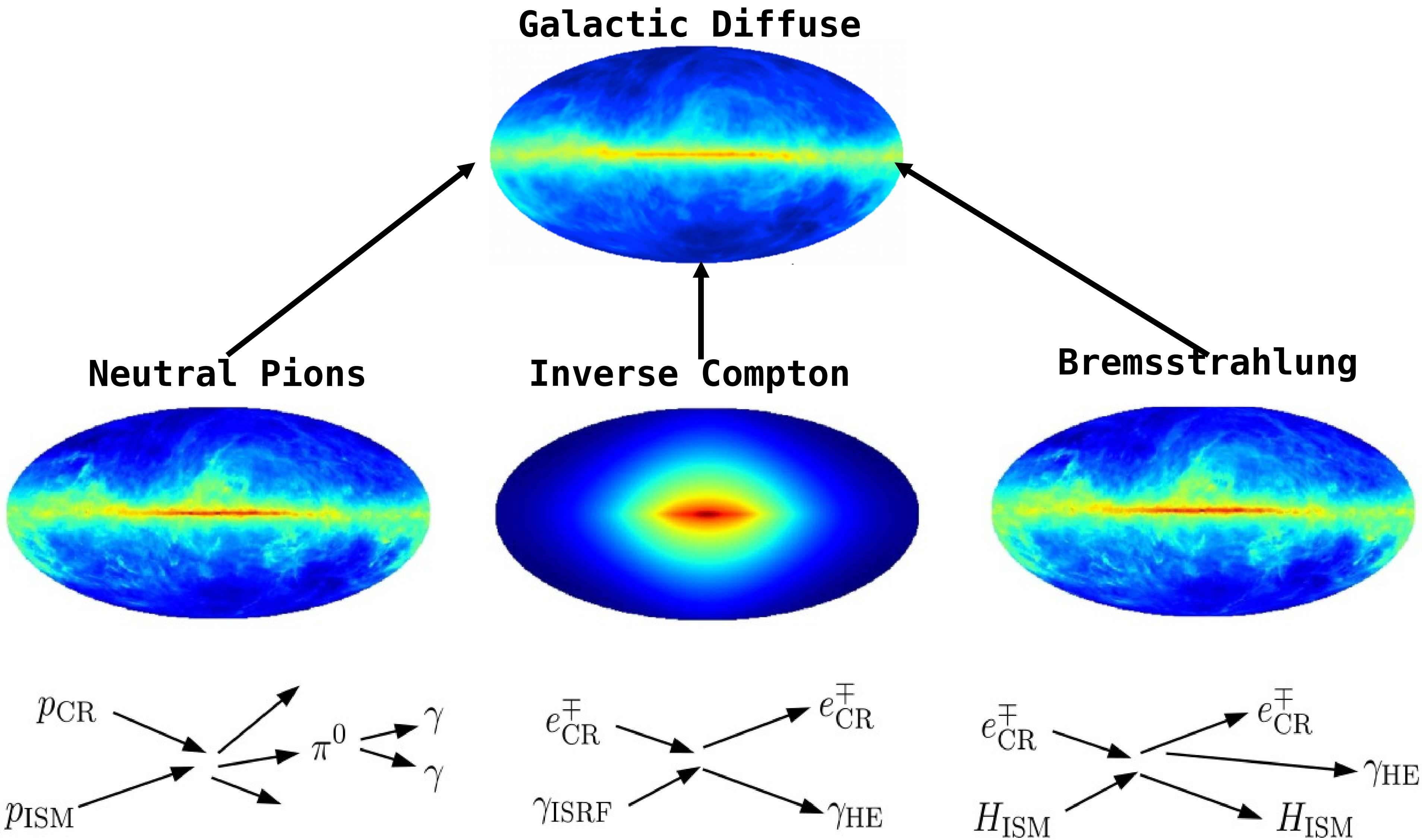

There are mainly two ways to model the Galactic diffuse emission

1) Empirical Method

- Uses a linear combination of gas column-densities and inverse Compton templates.
- Method used by the Fermi team to construct the official Galactic diffuse model.

2) Parametric Method

- Solves the diffusion Eq. (e.g. GALPROP, DRAGON).
- Allows physically motivated parameter choices.
- Harder to account for systematic uncertainties

There are mainly two ways to model the Galactic diffuse emission

1) Empirical Method

- Uses a linear comb[illegible]tion of gas c[illegible]-densities and [illegible]rse Compton templat[illegible]
- Method [illegible] by the Fermi [illegible] to construct th[illegible] official Galactic diffuse model.

2) Parametric Method

- Solves the diffusion Eq. (e.g. GALPROP, DRAGON).
- Allows physically motivated parameter choices.
- Harder to account for systematic uncertainties

Template fitting method

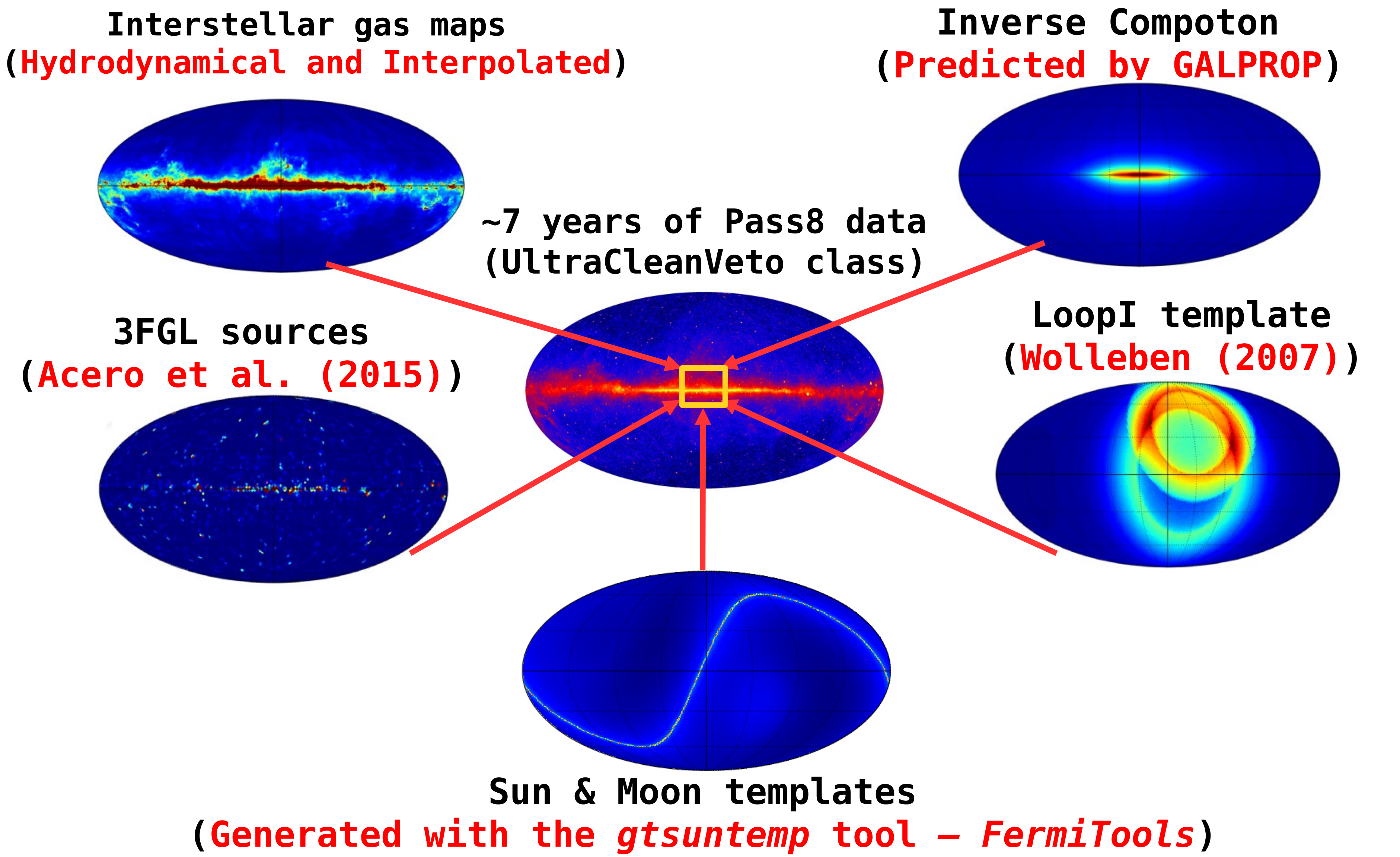

Atomic and Molecular Hydrogen

Gas correlated photons
(Neutral Pion and Bremsstrahlung)

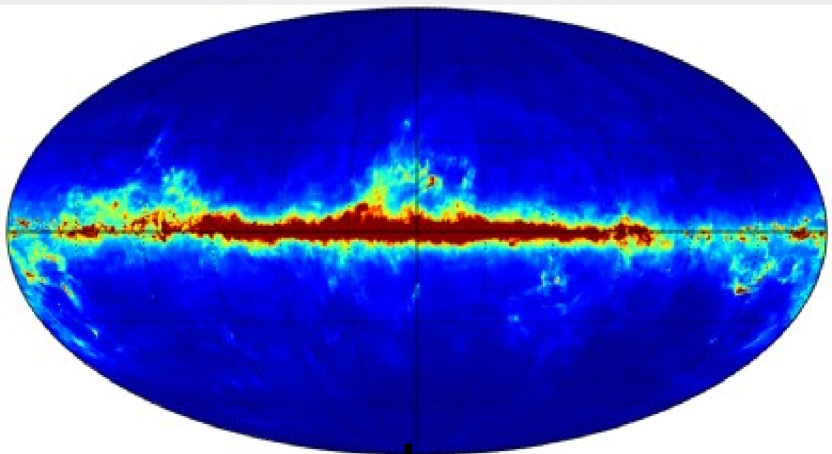

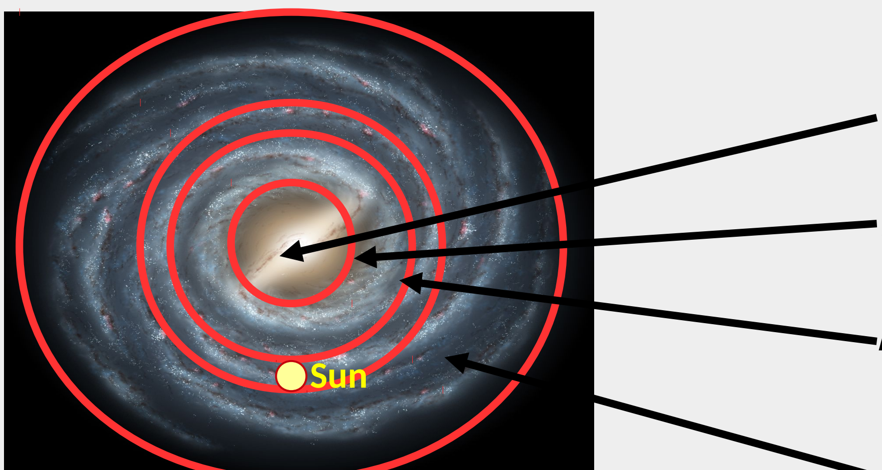

Image credit: Robert Hurt, JPL

Atomic and Molecular Hydrogen

Image Credit:http://spiff.rit.edu/classes/phys230/lectures/ism_gas/ism_gas.html

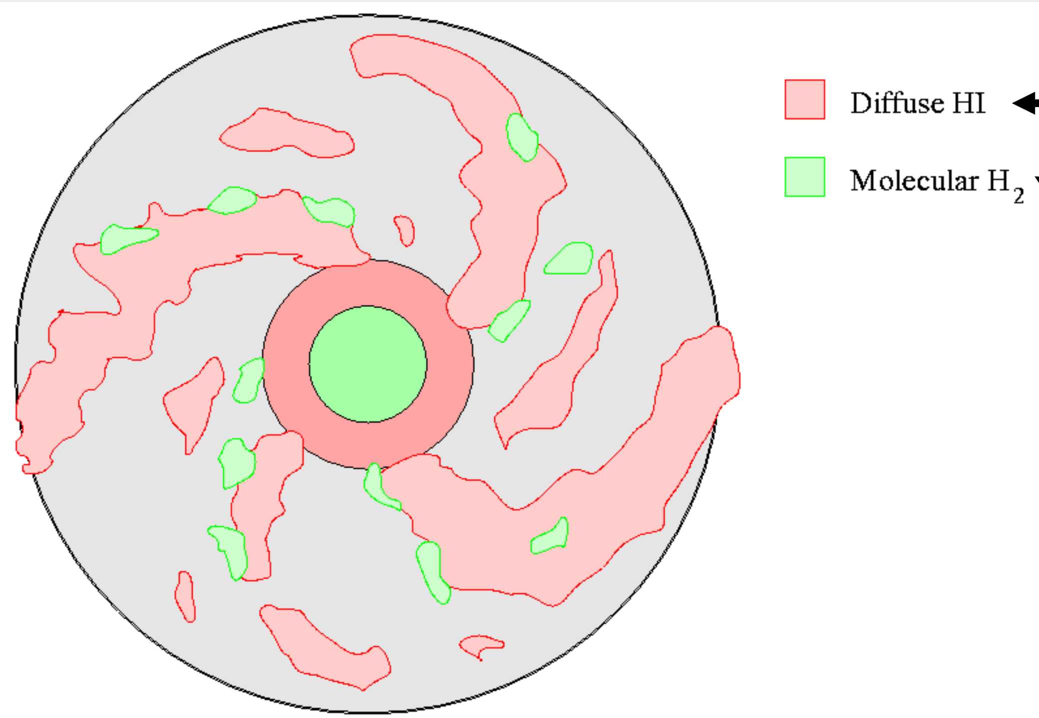

LAB Survey [Kalberla et.al.(2005)]

Center for Astrophysics [Damae et.al.(2000)]

HI is measured with 21-cm emission
H2 is traced by 2.6-mm line emission of CO

Annulii gas decomposition

Image Credit:http://spiff.rit.edu/classes/phys230/lectures/ism_gas/ism_gas.html

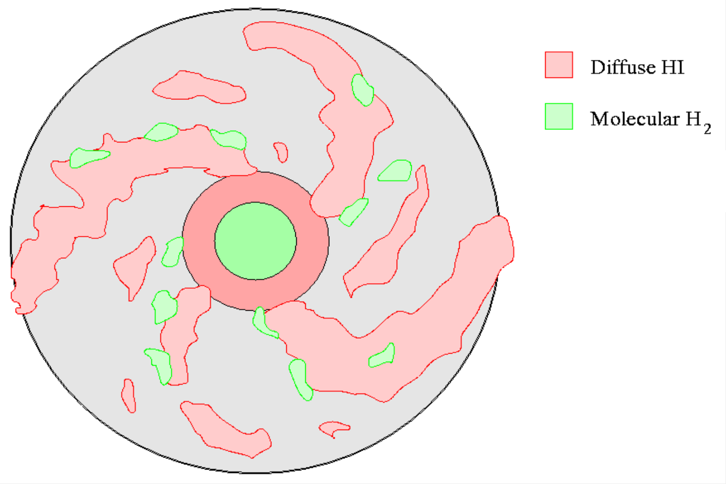

Astronomical Surveys

Gas Cloud Velocity

Gas Cloud Temperature

Annulii gas decomposition

Image Credit:http://spiff.rit.edu/classes/phys230/lectures/ism_gas/ism_gas.html

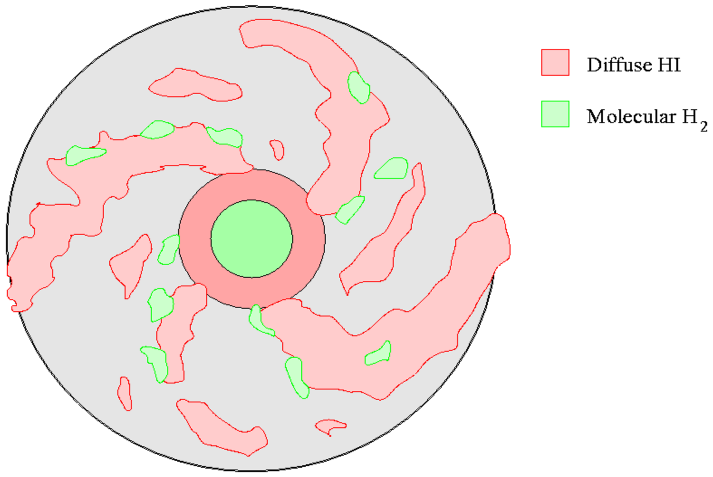

Image Credit:http://www.cv.nrao.edu/course/astr534/HILine.html

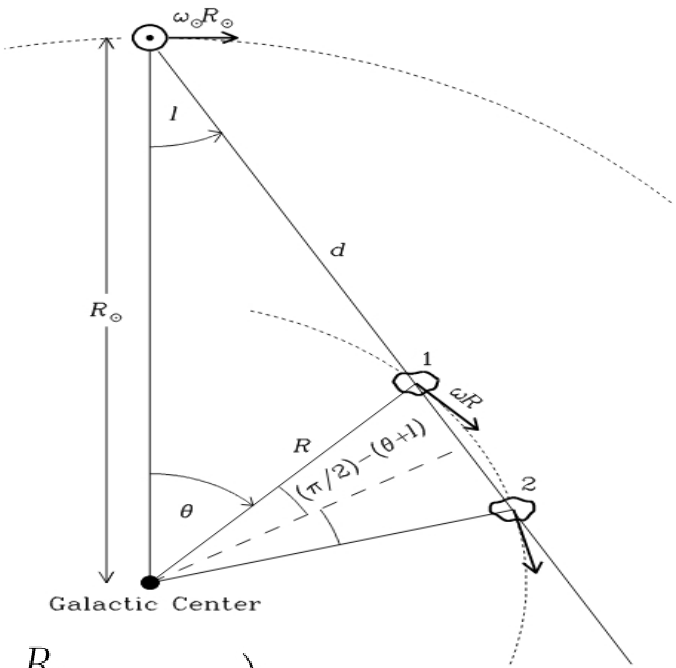

Astronomical Surveys

Gas Cloud Velocity

$$V_{\rm LSR} = \left(V(R)\frac{R_\odot}{R} - V(R_\odot)\right)\sin(l)\cos(b),$$

Gas Cloud distance

Gas Cloud Temperature

Annulii gas decomposition

Image Credit:http://spiff.rit.edu/classes/phys230/lectures/ism_gas/ism_gas.html

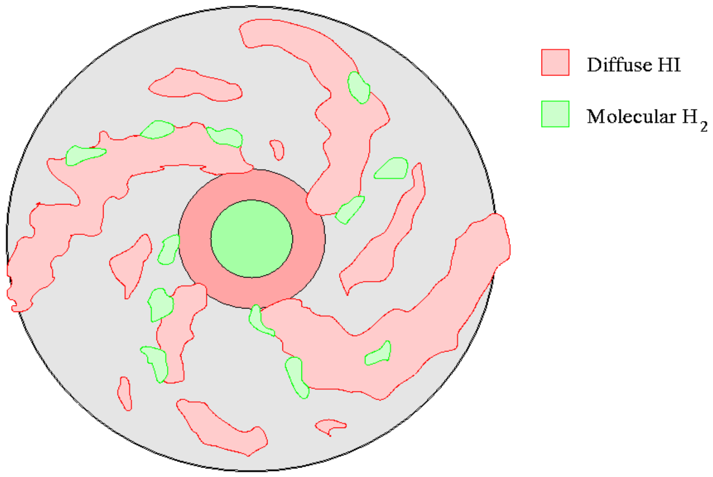

Image Credit:http://www.cv.nrao.edu/course/astr534/HILine.html

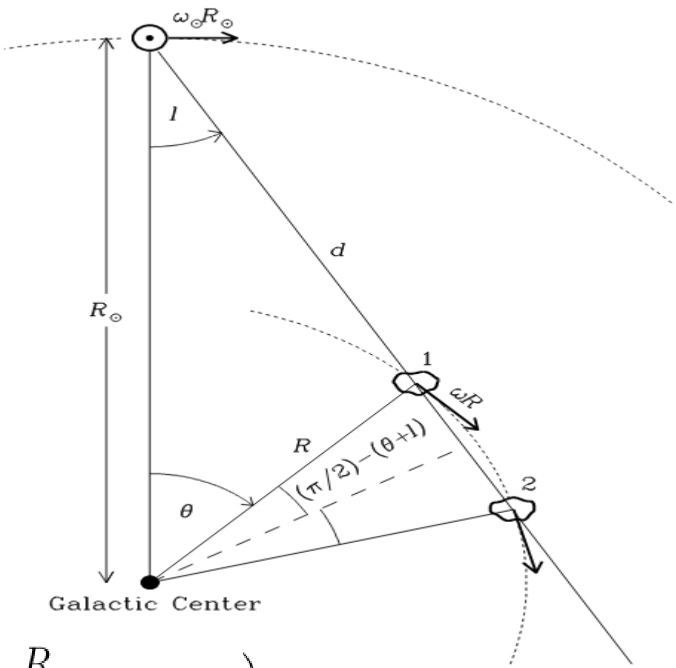

Astronomical Surveys

$$V_{\rm LSR} = \left(V(R)\frac{R_\odot}{R} - V(R_\odot)\right)\sin(l)\cos(b),$$

Gas Cloud Velocity → **Gas Cloud distance**

$$N(HI) = -C\,T_s \int dv \log\left(1 - \frac{T_B(v)}{T_s - T_{\rm bg}}\right)$$

Gas Cloud Temperature → **Gas Cloud density**

Annulii gas decomposition

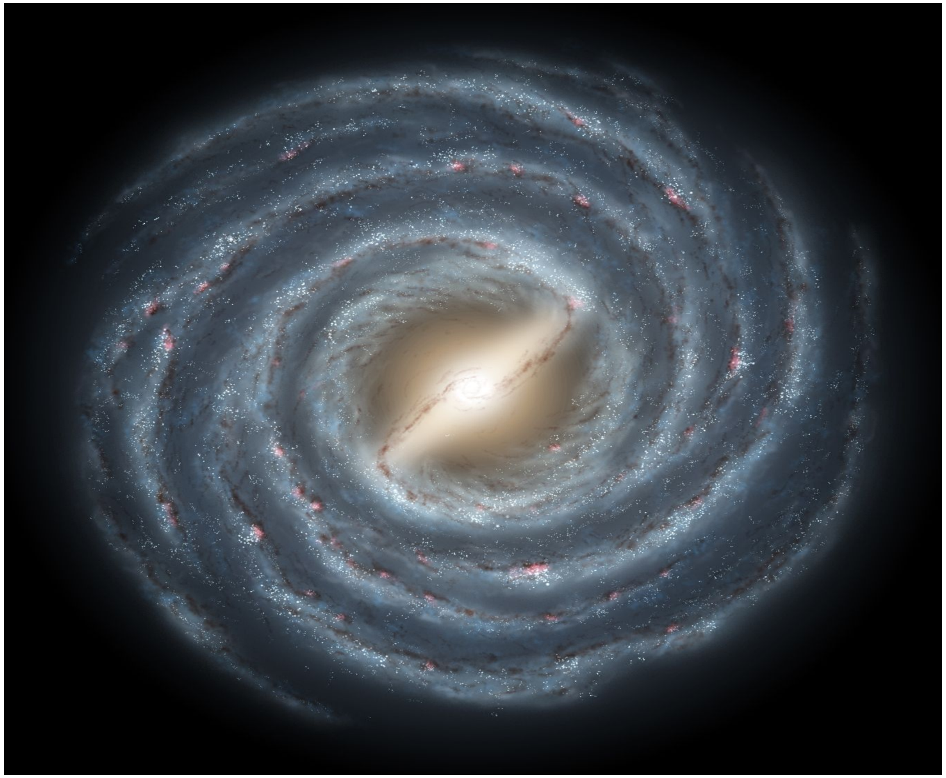

Image credit: Robert Hurt, JPL

Image Credit:http://www.cv.nrao.edu/course/astr534/HILine.html

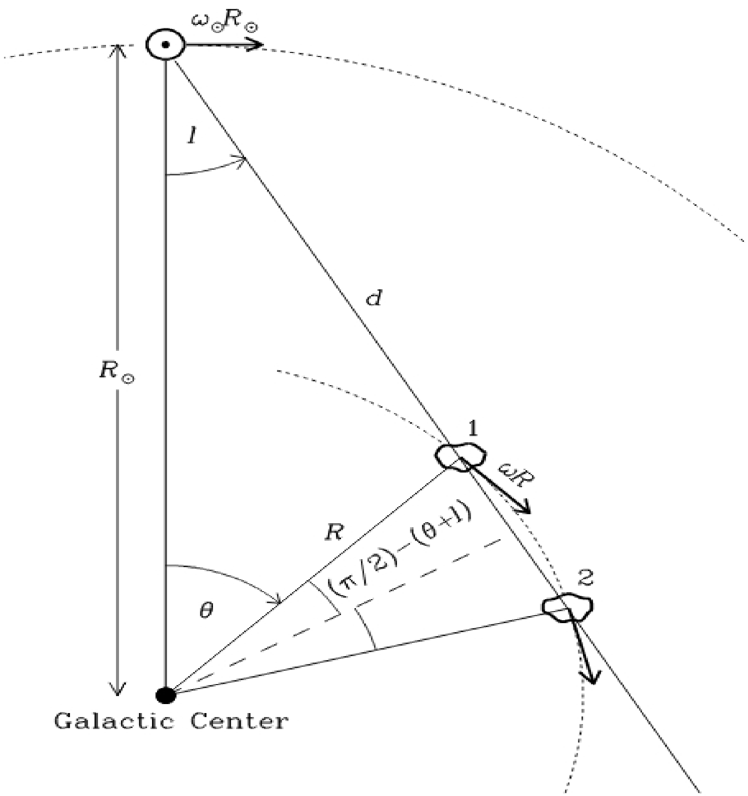

The assumption of circular motion toward the Galactic Center is incorrect!

(1) Interpolation Method

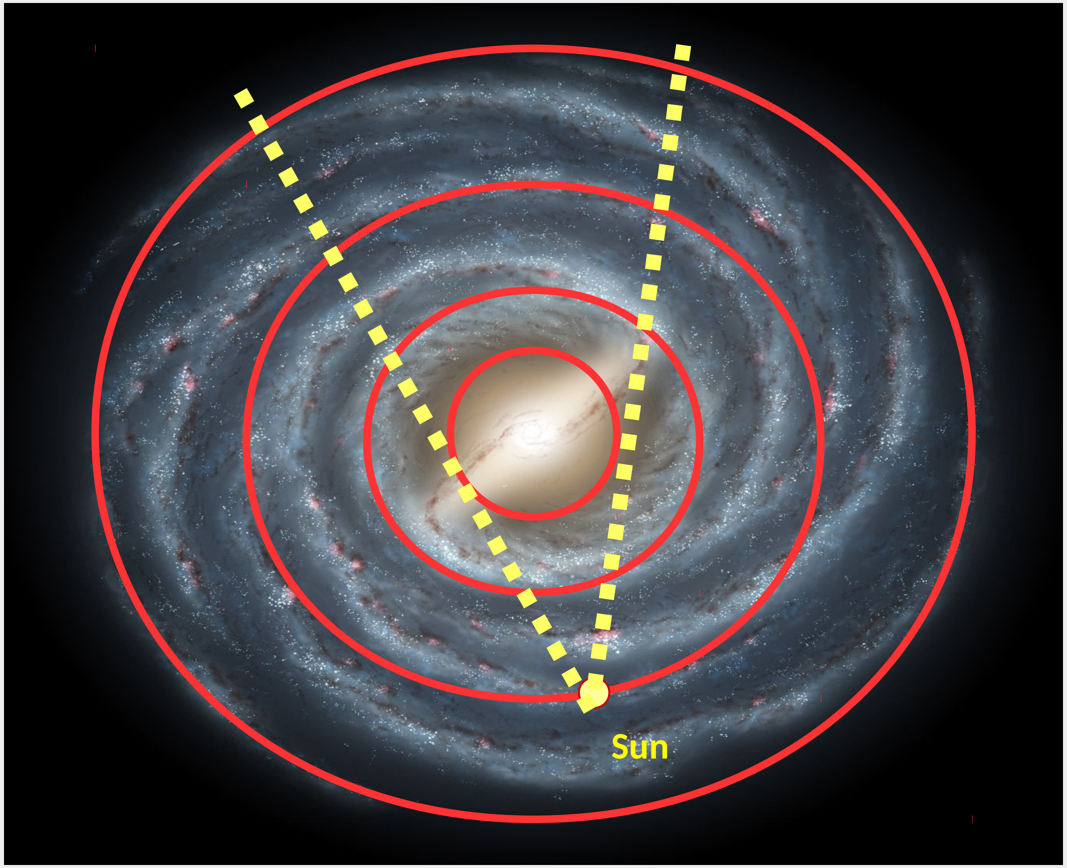

Image credit: Robert Hurt, JPL

Fermi-LAT uses an interpolation to estimate the ISM gas for 10>longitude>-10 degrees.

(2) Hydrodynamical Simulations (this work)

Image Credit:http://spiff.rit.edu/classes/phys230/lectures/ism_gas/ism_gas.html

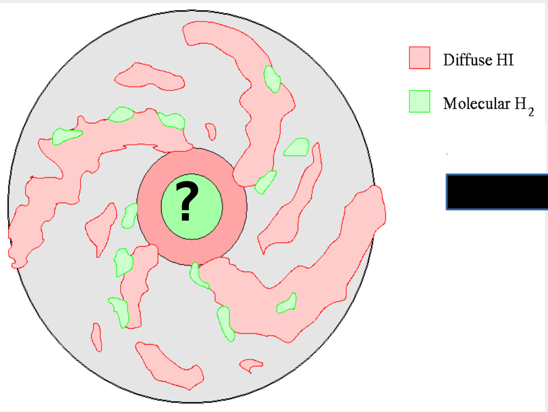

Pohl et al. (2007)

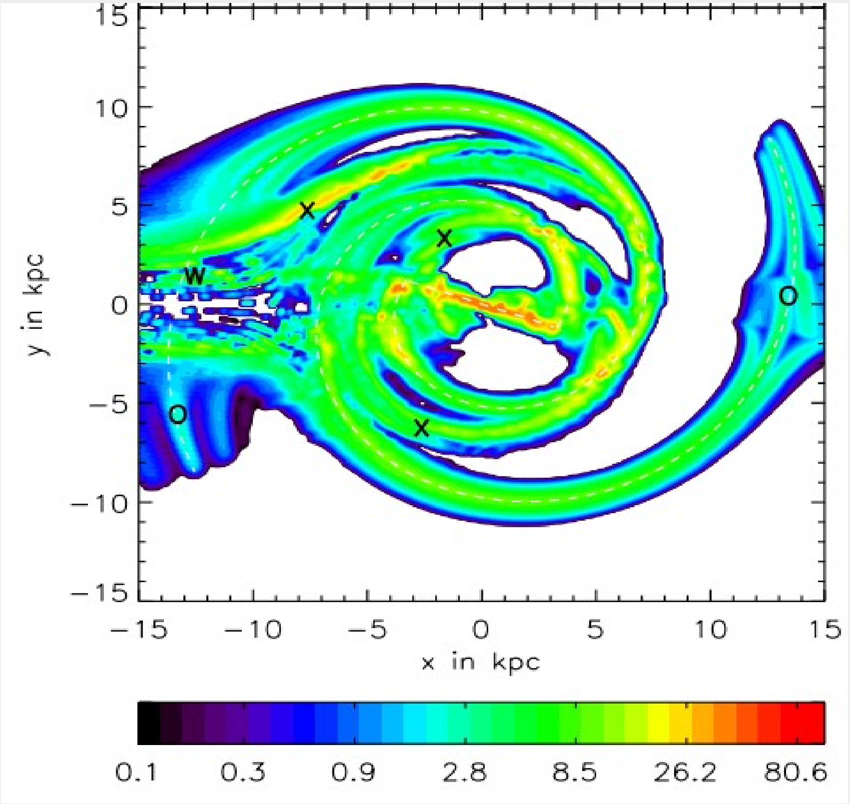

Hydrodynamical simulations provide kinematic resolution toward the Galactic Center.

Interpolated vs Hydrodynamical method

Macias et al. Nat. Astr.(2018)

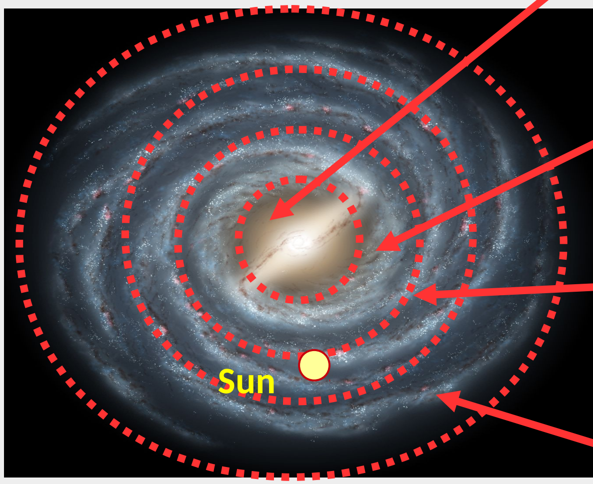

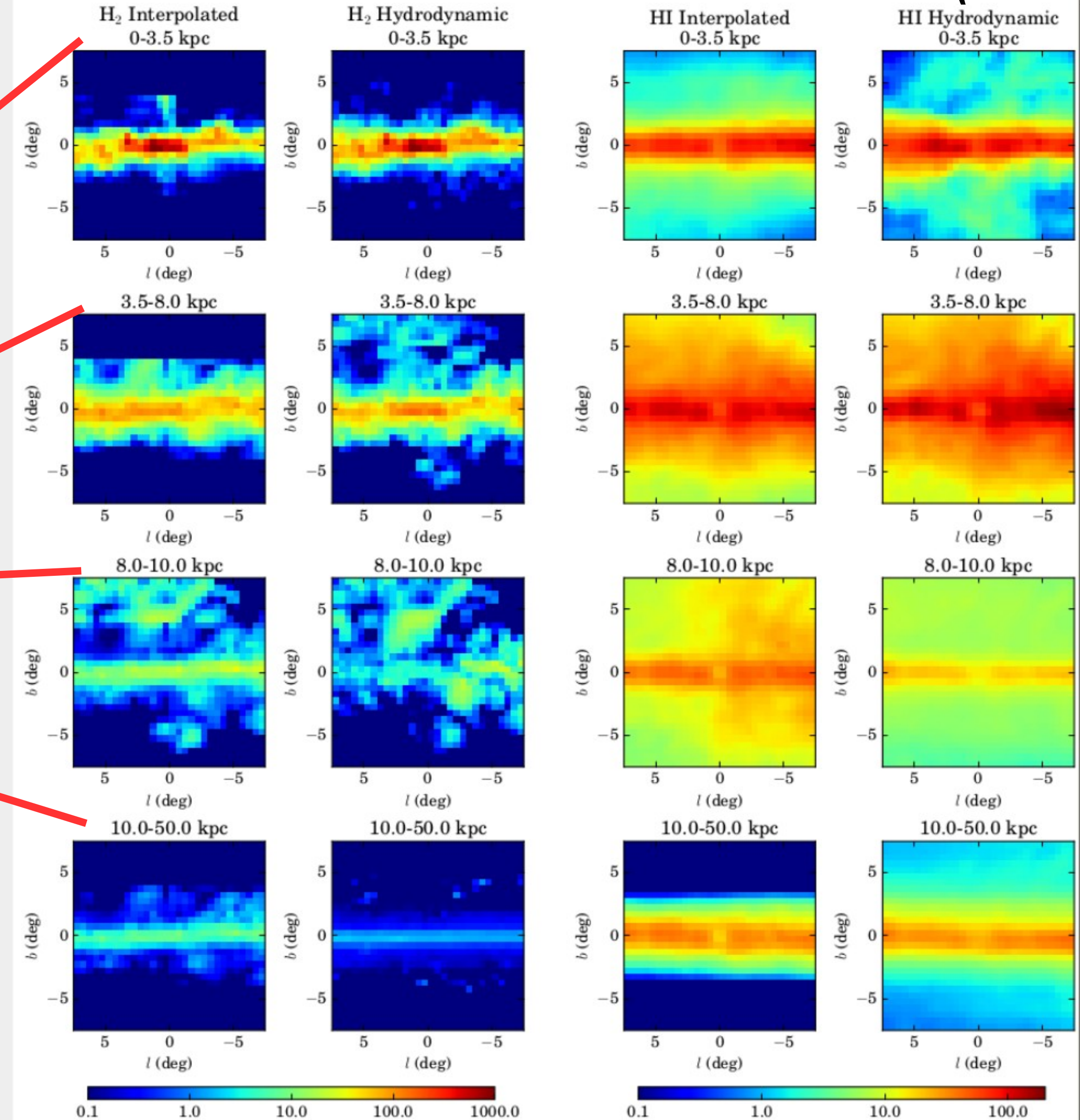

There are noticeable morphological differences between the two methods.

Interpolated vs Hydrodynamical method

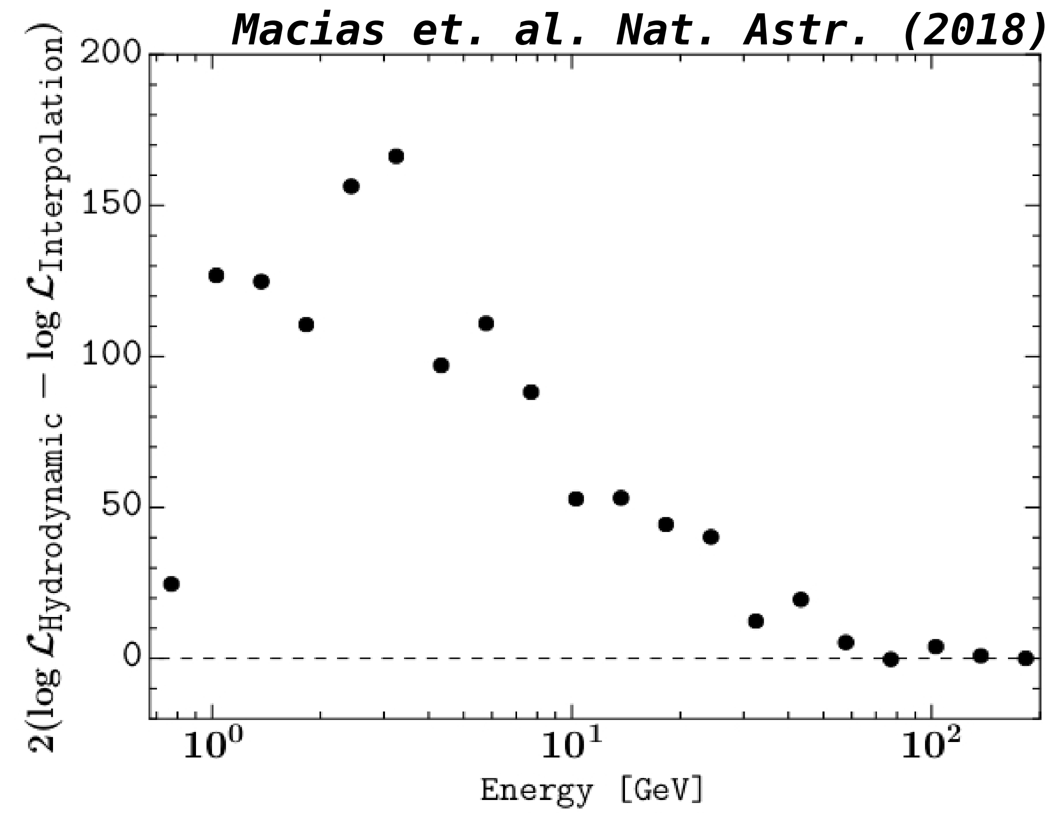

The hydrodynamical gas map is better than the interpolated one with a significance of 35σ

New point source candidates in the ROI

Macias et al. (2018)

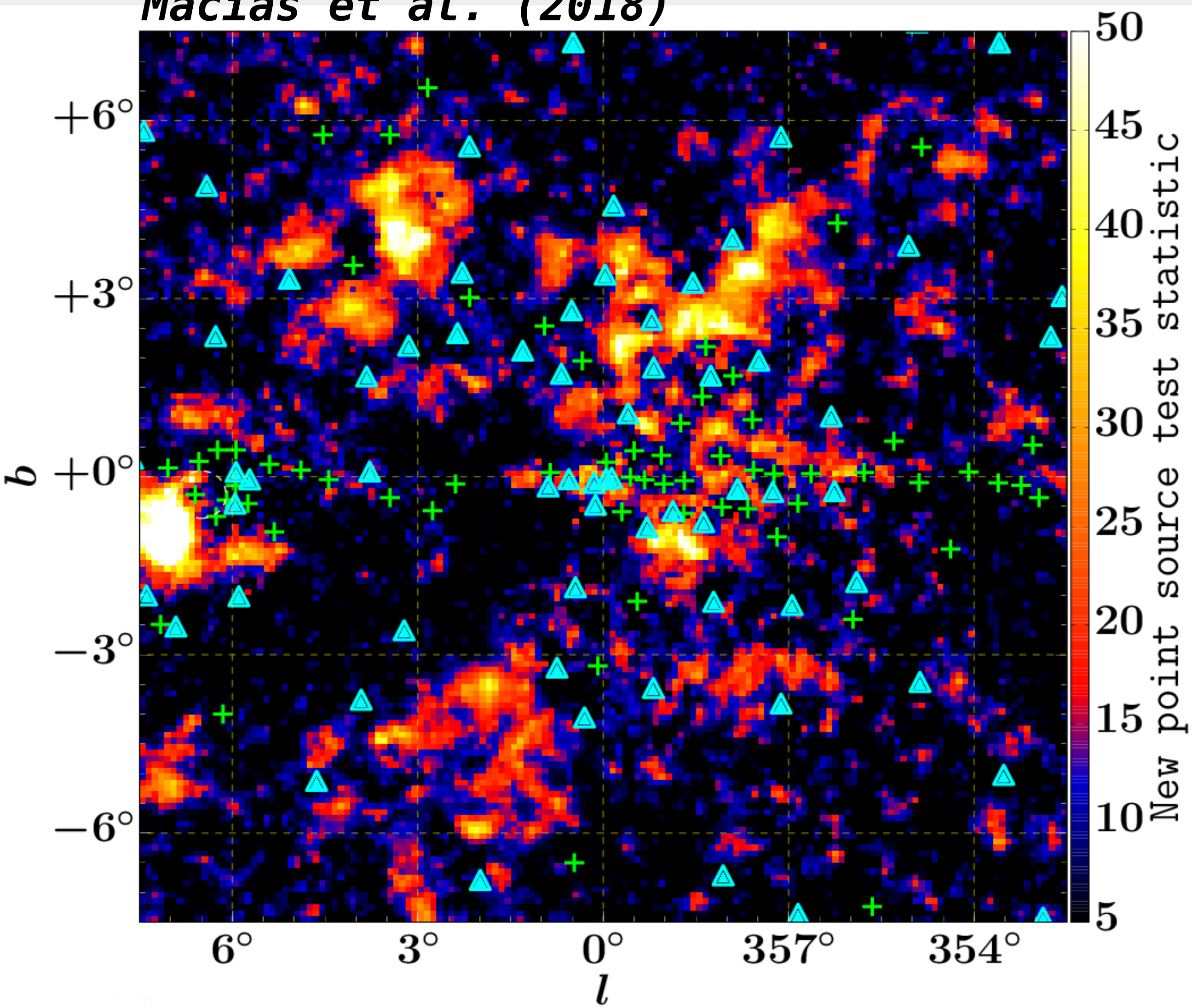

3FGL
New point source candidates

Detection threshold:
TS > 41.8
(for 19 d.o.f.)

Found **64 gamma-ray point source candidates**
in the inner 15x15 deg RoI of the Galactic Center

Comparison with new point sources in 2FIG

Macias et al. (2018)

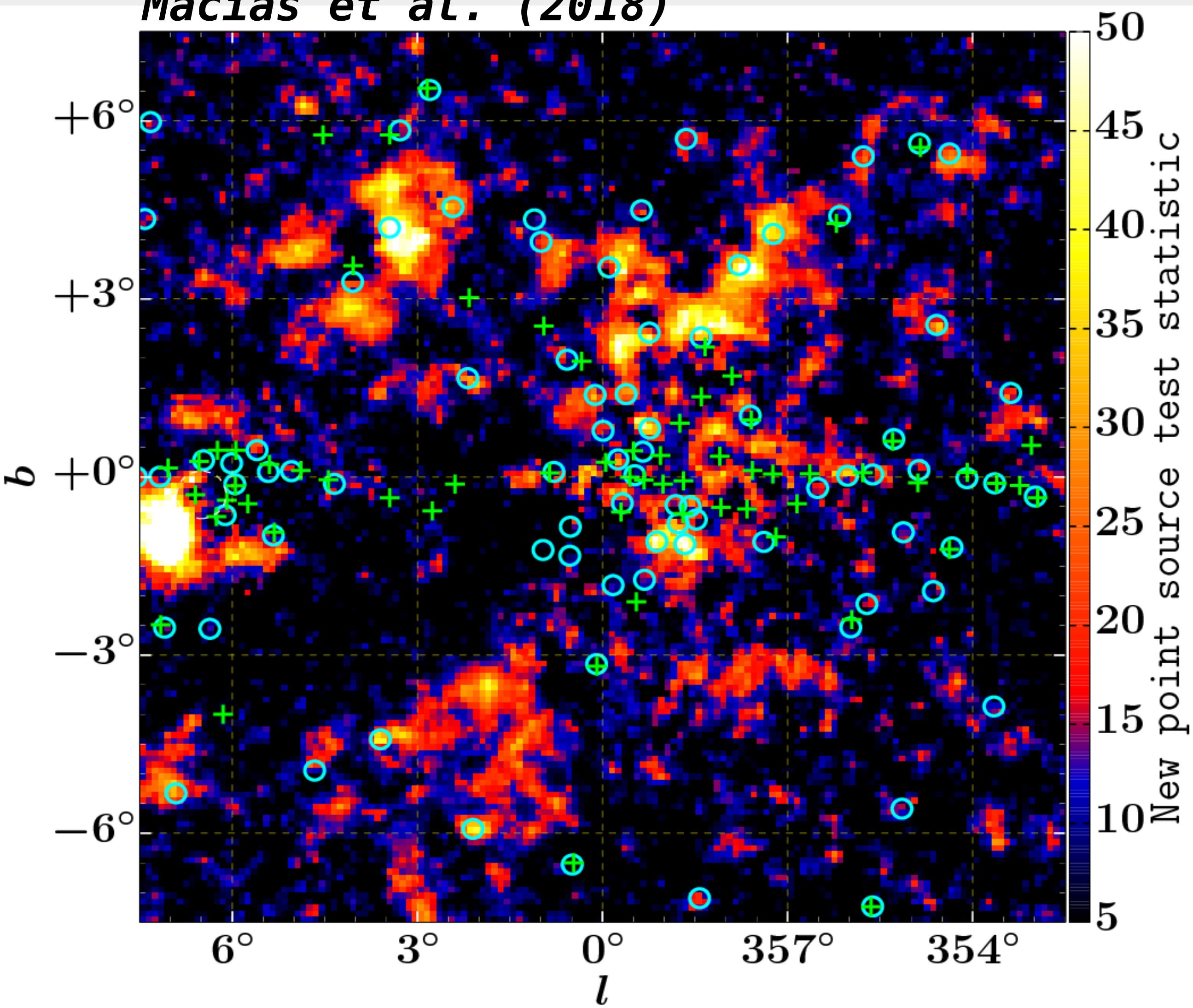

2FIG
This work

There are 81 new point sources in 2FIG and 64 in our work. Our analysis confirms 31 2FIG PSs.

The X-shaped Stellar Population of the Galactic Bulge

- Close to 33% of all Galaxies display a boxy/peanut or X-shape bulge when seen edge on [Jarvis 1986].

The peanut-shaped Stellar Population of the Galactic Bulge

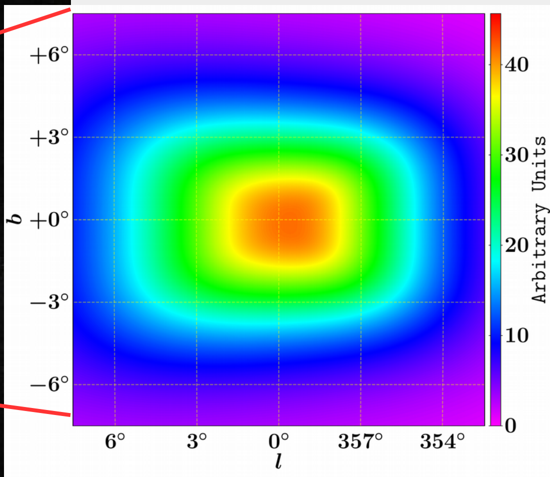

Freudenreich (1998)

There is a peanut shaped excess in infrared emission as seen by the COBE satellite.

The peanut-shaped Stellar Population of the Galactic Bulge

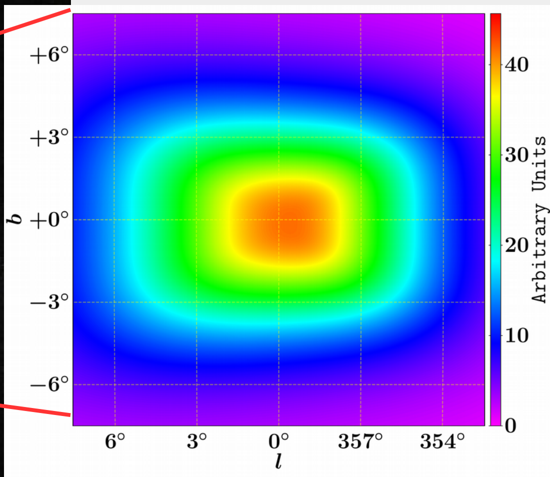

Freudenreich (1998)

Dynamical instabilities of stars in the Galactic bar send these to orbits resembling a peanut shape

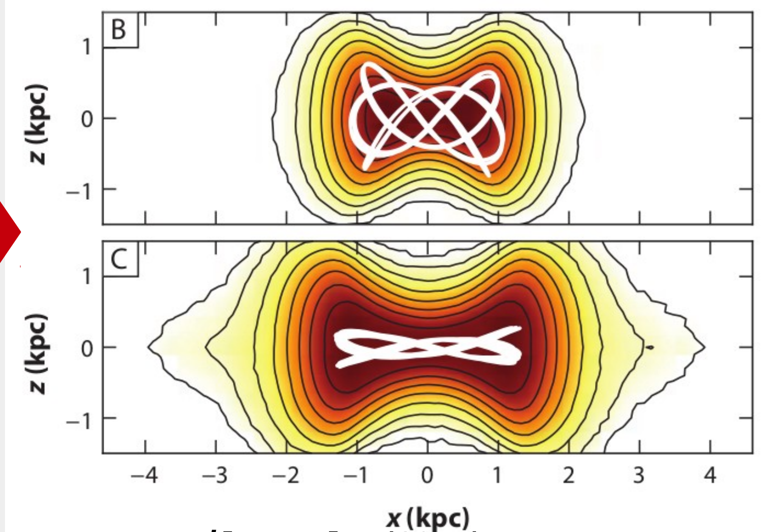

Portail et al. (2015)
Bland-Hawthorn & Gerhard (2016)

The Peanut-shaped Stellar Population of the Galactic Bulge and the Nuclear bulge stars

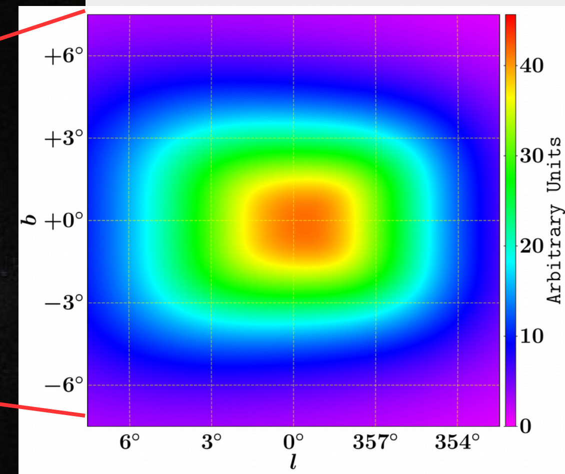

Ness and Lang (2016)
Macias et al. (2016)

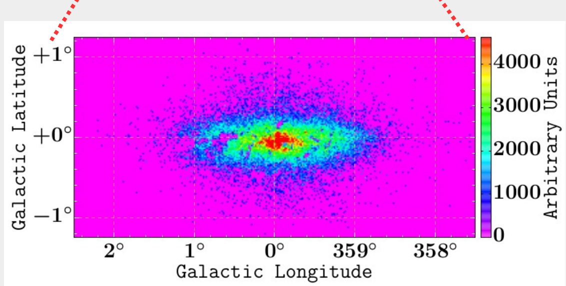

Nishiyama et al (2013) – observed with the SIRIUS near-infrared camera (NAOJ).

There is an additional dense and disky star population close to the supermassive black hole.

Add new components systematically

Base	Source	$\log(\mathcal{L}_{\rm Base})$	$\log(\mathcal{L}_{\rm Base+Source})$	$\mathrm{TS}_{\rm Source}$	σ	Number of source parameters
baseline	FB	-172461.4	-172422.3	78	6.9	19
baseline	NFW-s	-172461.4	-172265.3	392	18.4	19
baseline	Boxy bulge	-172461.4	-172238.7	445	19.7	19
baseline	X-bulge	-172461.4	-172224.1	475	20.5	19
baseline	NFW	-172461.4	-172167.9	587	23.0	19
baseline	NB	-172461.4	-171991.8	939	29.5	19
baseline	NP	-172461.4	-169804.1	5315	55.7	64×19
baseline+NP	FB	-169804.1	-169773.6	61	5.8	19
baseline+NP	NB	-169804.1	-169697.2	214	13.0	19
baseline+NP	Boxy bulge	-169804.1	-169663.7	281	15.3	19
baseline+NP	NFW	-169804.1	-169623.3	362	17.6	19
baseline+NP	X-bulge	-169804.1	-169616.2	376	18.0	19
baseline+NP+Boxy bulge	NFW	-169663.7	-169598.2	131	9.7	19
baseline+NP+Boxy bulge	NB	-169663.7	-169566.0	195	12.4	19
baseline+NP+Boxy bulge+NB	NFW	-169566.0	-169553.3	25	2.7	19
baseline+NP+Boxy bulge+NFW	NB	-169598.2	-169553.3	90	7.6	19
baseline+NP+NFW	Boxy bulge+NB	-169623.3	-169553.0	140	10.0	2×19
baseline+NP+NFW	X-bulge+NB	-169623.3	-169531.0	185	10.8	2×19
baseline+NP+NB	X-bulge	-169697.2	-169542.0	310	16.1	19
baseline+NP+NB	Boxy bulge	-169697.2	-169566.0	262	14.6	19
baseline+NP+NB	NFW	-169697.2	-169599.0	197	12.4	19
baseline+NP+NB+NFW	X-bulge	-169598.9	-169531.0	136	9.9	19
baseline+NP+X-bulge+NB	NFW	-169542.0	-169531.0	22	2.4	19

Gas + IC + 3FGL + Loop I + Sun & Moon

➔ **NFW detected at low significance when bulge is included**

Macias et al (2018)

Add new components systematically

Gas + IC +
3FGL + Loop I
+ Sun & Moon

Base	Source	$\log(\mathcal{L}_{\text{Base}})$	$\log(\mathcal{L}_{\text{Base+Source}})$	$\text{TS}_{\text{Source}}$	σ	Number of source parameters
baseline	FB	-172461.4	-172422.3	78	6.9	19
baseline	NFW-s	-172461.4	-172265.3	392	18.4	19
baseline	Boxy bulge	-172461.4	-172238.7	445	19.7	19
baseline	X-bulge	-172461.4	-172224.1	475	20.5	19
baseline	NFW	-172461.4	-172167.9	587	23.0	19
baseline	NB	-172461.4	-171991.8	939	29.5	19
baseline	NP	-172461.4	-169804.1	5315	55.7	64×19
baseline+NP	FB	-169804.1	-169773.6	61	5.8	19
baseline+NP	NB	-169804.1	-169697.2	214	13.0	19
baseline+NP	Boxy bulge	-169804.1	-169663.7	281	15.3	19
baseline+NP	NFW	-169804.1	-169623.3	362	17.6	19
baseline+NP	X-bulge	-169804.1	-169616.2	376	18.0	19
baseline+NP+Boxy bulge	NFW	-169663.7	-169598.2	131	9.7	19
baseline+NP+Boxy bulge	NB	-169663.7	-169566.0	195	12.4	19
baseline+NP+Boxy bulge+NB	NFW	-169566.0	-169553.3	25	2.7	19
baseline+NP+Boxy bulge+NFW	NB	-169598.2	-169553.3	90	7.6	19
baseline+NP+NFW	Boxy bulge+NB	-169623.3	-169553.0	140	10.0	2×19
baseline+NP+NFW	X-bulge+NB	-169623.3	-169531.0	185	10.8	2×19
baseline+NP+NB	X-bulge	-169697.2	-169542.0	310	16.1	19
baseline+NP+NB	Boxy bulge	-169697.2	-169566.0	262	14.6	19
baseline+NP+NB	NFW	-169697.2	-169599.0	197	12.4	19
baseline+NP+NB+NFW	X-bulge	-169598.9	-169531.0	136	9.9	19
baseline+NP+X-bulge+NB	NFW	-169542.0	-169531.0	22	2.4	19

➔ NFW detected at low significance when bulge is included

Macias et al (2018)

Systematics

Gas maps: using the gas maps used by the Fermi Diffuse models yield the same conclusions

Point sources: using none or the 2FIG point source catalog yield the same conclusions

Base	Source	$\log(\mathcal{L}_{\mathrm{Base}})$	$\log(\mathcal{L}_{\mathrm{Base+Source}})$	$\mathrm{TS}_{\mathrm{Source}}$	σ	Number of source parameters
baseline+NB+Boxy	NFW	-172005.9	-171999.0	13.8	1.4	19
baseline+NFW	NB+Boxy	-172167.9	-171999.0	337.8	18.3	2×19
baseline*	NFW	-173565.0	-172929.2	1272	34.6	19
baseline*+NFW	NB+Boxy	-172929.2	-172533.0	792.4	28.2	2×19
baseline*+NB+Boxy	NFW	-172547.4	-172533.0	28.8	3.0	19
baseline	2FIG	-172461.4	-170710.5	3501	37.3	81×19
baseline+2FIG	Boxy	-170710.5	-170536.3	348.4	18.7	19
baseline+2FIG	NFW	-170710.5	-170484.6	452	19.9	19
baseline+2FIG	NB	-170710.5	-170470.5	480	20.6	19
baseline+2FIG+NB	NFW	-170470.5	-170387.8	165	11.1	19
baseline+2FIG+NB	Boxy	-170470.5	-170317.2	306.6	17.5	19
baseline+2FIG+NB+Boxy	NFW	-170317.2	-170313.5	7.4	0.5	19

Galactic plane mask: using a |b| < 1 deg mask yields the same conclusions

baseline	NFW	-430824.6	-430696.9	255	14.4	19
baseline	Boxy	-430824.6	-430626.1	397	18.5	19
baseline	NP	-430824.6	-430189.9	1269	35.6	22×19
baseline+NP	NFW	-430189.9	-430097.0	186	12.0	19
baseline+NP	Boxy	-430189.9	-430035.8	308	16.1	19
baseline+NP+Boxy	NFW	-430035.8	-430026.3	19	2.0	19

Bulge preferred over spherical symmetry

Bulge over NFW²

When a bulge model is included, the detection of NFW² falls (<3σ) while bulge significance is ~10σ .

This is robust to

- 1. Point sources used.
- 2. Diffuse emission models used.
- 3. Galactic mask.

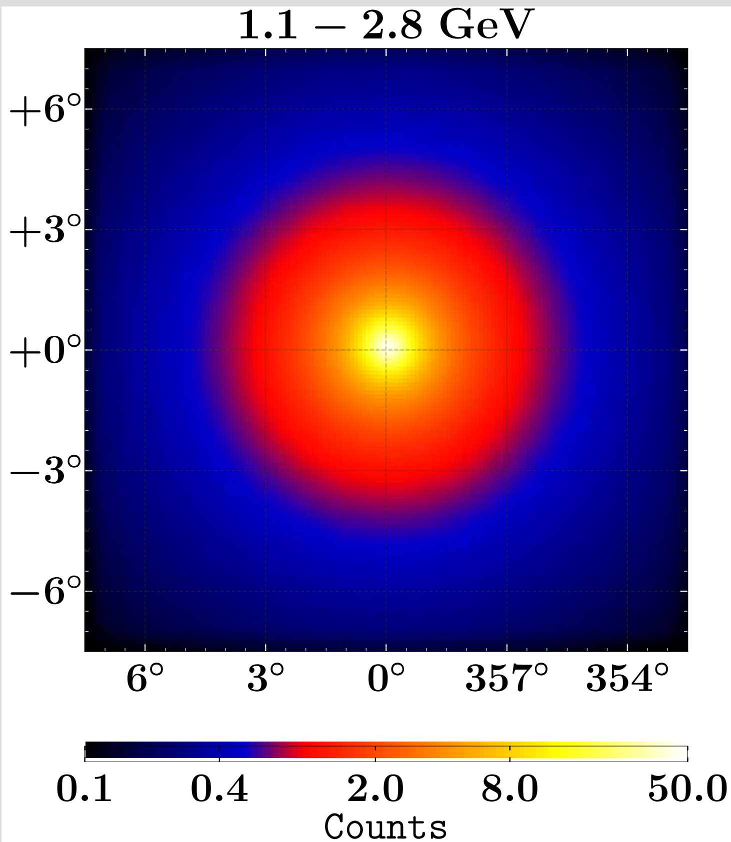

<<

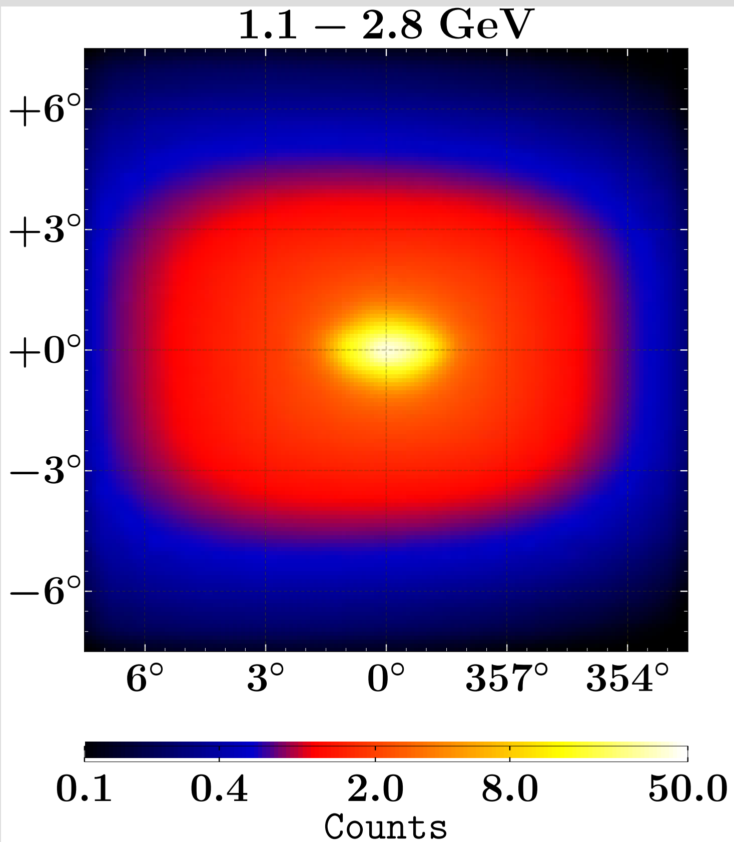

Spectrum of the peanut bulge component is consistent with previous GCE results

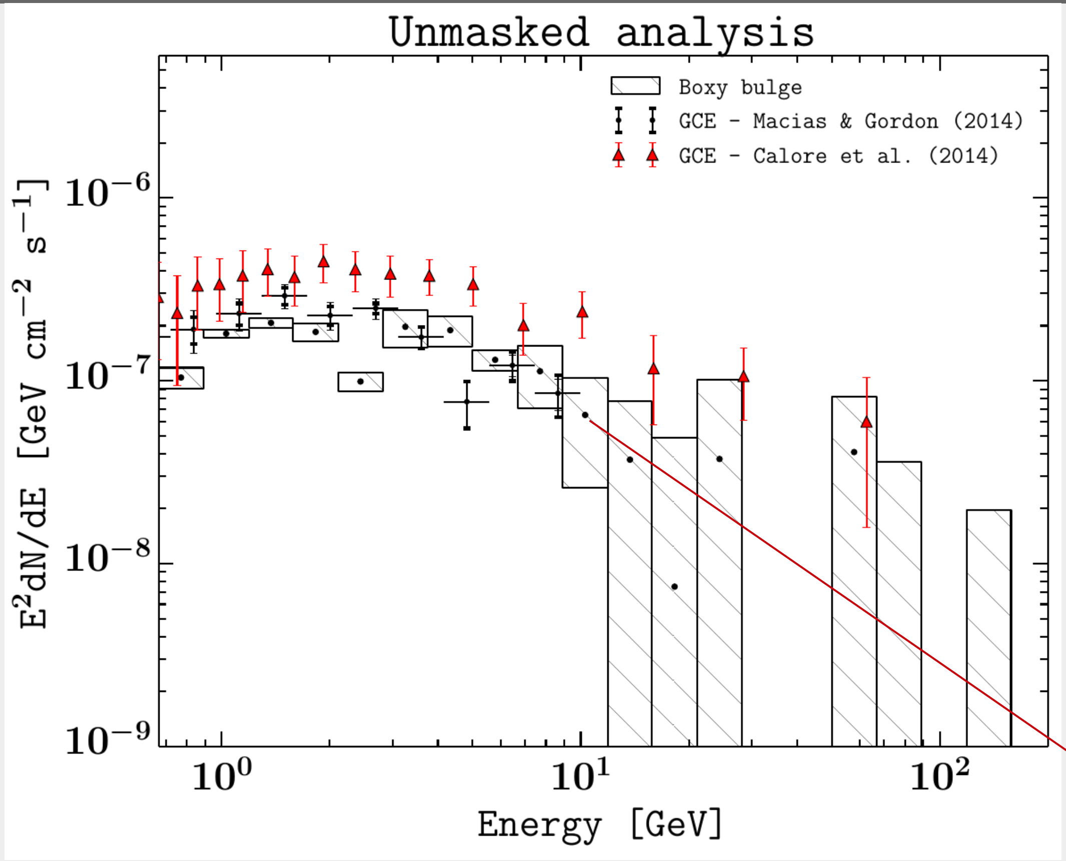

$$\frac{dN}{dE} \propto E^{-2.1\pm0.1}\exp\left(-\frac{E}{15\pm6\ \mathrm{GeV}}\right)$$

$$\mathrm{L} = (7.8\pm0.8)\times10^{36}\ \mathrm{erg/s}$$

Spectrum of the GCE consistent with MSPs in Globular Clusters

Millisecond pulsars

- Millisecond pulsars are gamma-ray sources with similar spectra to the GCE.
- *O*(5,000) needed in the Galactic Center

Globular clusters detected in gamma rays

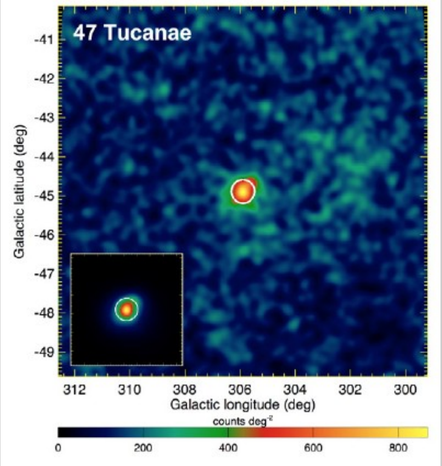

Fermi (2010)

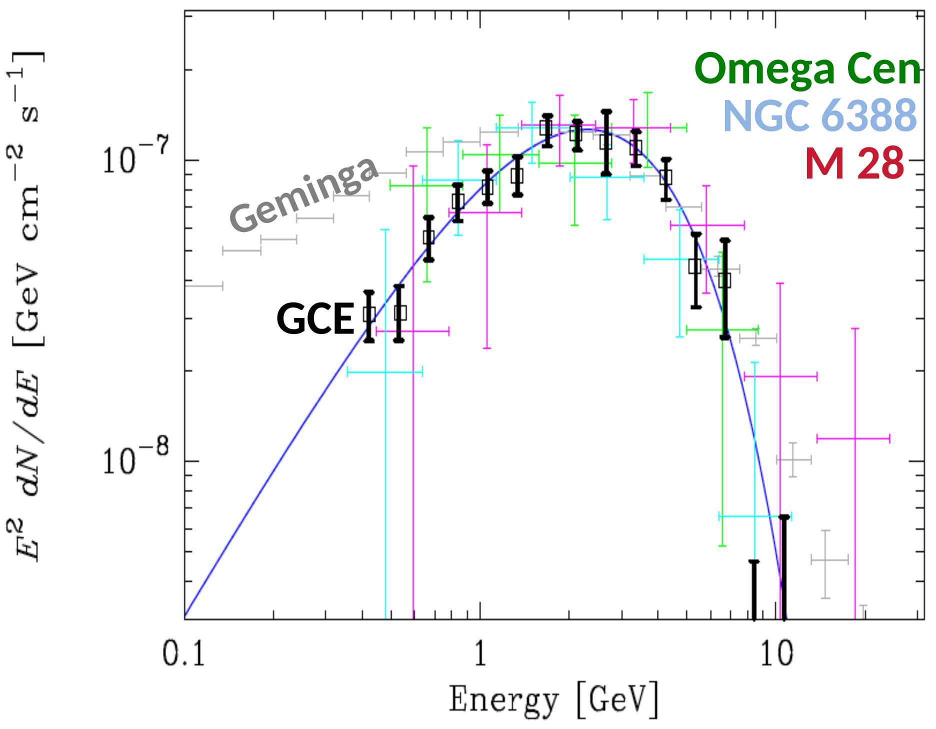

Abazajian (2011)

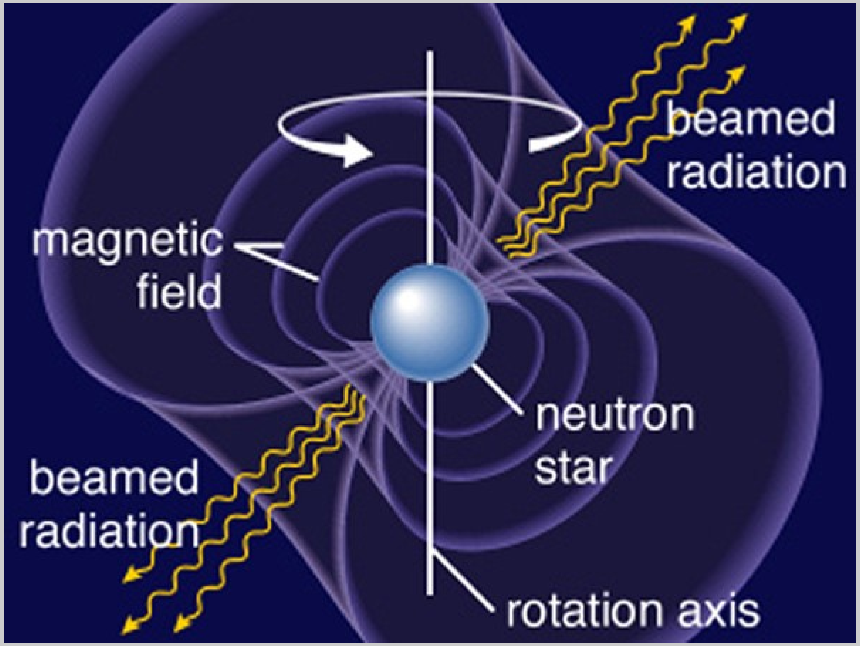

An unresolved population of Millisecond pulsars traced by the peanut bulge and nuclear bulge could explain the Fermi GeV excess

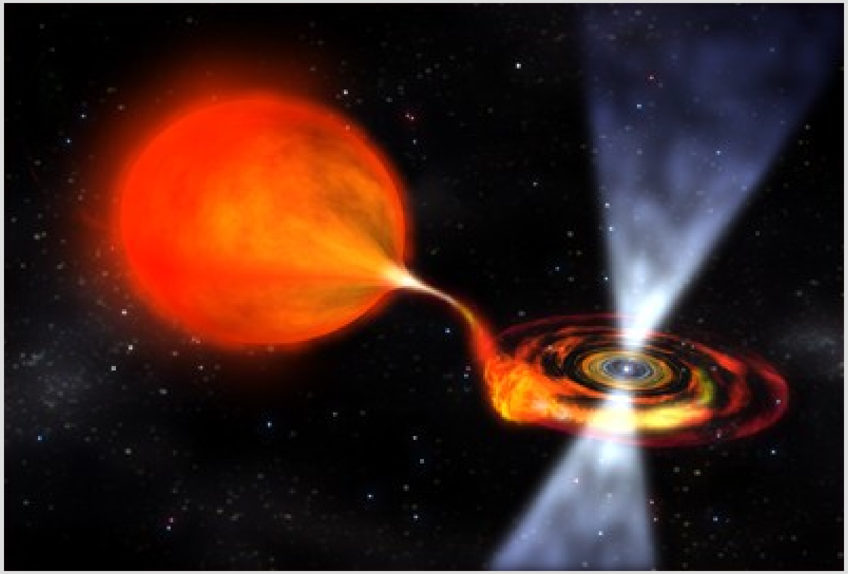

Image Credit: NASA/Dana Berry.

Luminosity-to-mass ratio

Entire Galaxy → $\sim 2 \times 10^{27}\ \mathrm{erg/s}/M_\odot$

Galactic bulge → $\sim 3 \times 10^{27}\ \mathrm{erg/s}/M_\odot$

47 Tuc → $\sim 5 \times 10^{28}\ \mathrm{erg/s}/M_\odot$

Independent confirmation of our results

SkyFACT = **Sky F**actorization with **A**daptive **C**onstrained **T**emplates

Hybrid method to study diffuse gamma rays that combines adaptive spatial-spectral template regression and image reconstruction.

Storm et al (2017)

$$\phi_{pb} = \sum_k T_p^{(k)} \tau_p^{(k)} \cdot S_b^{(k)} \sigma_b^{(k)} \cdot \nu^{(k)}$$

Modulated by nuisance parameters τ, σ, ν

Spatial template Spectral template

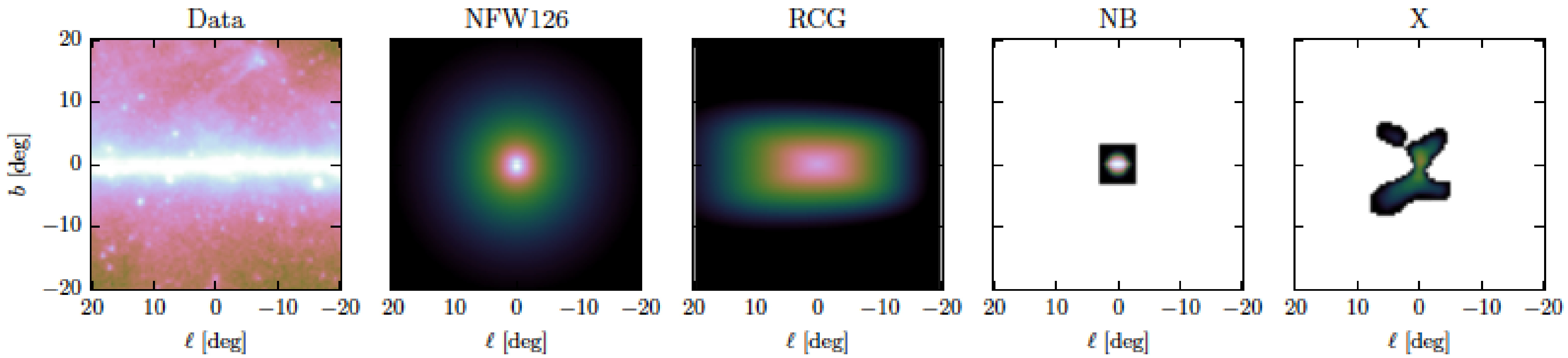

Bartels et. al. Nat. Astr. (2018)

Independent confirmation of our results

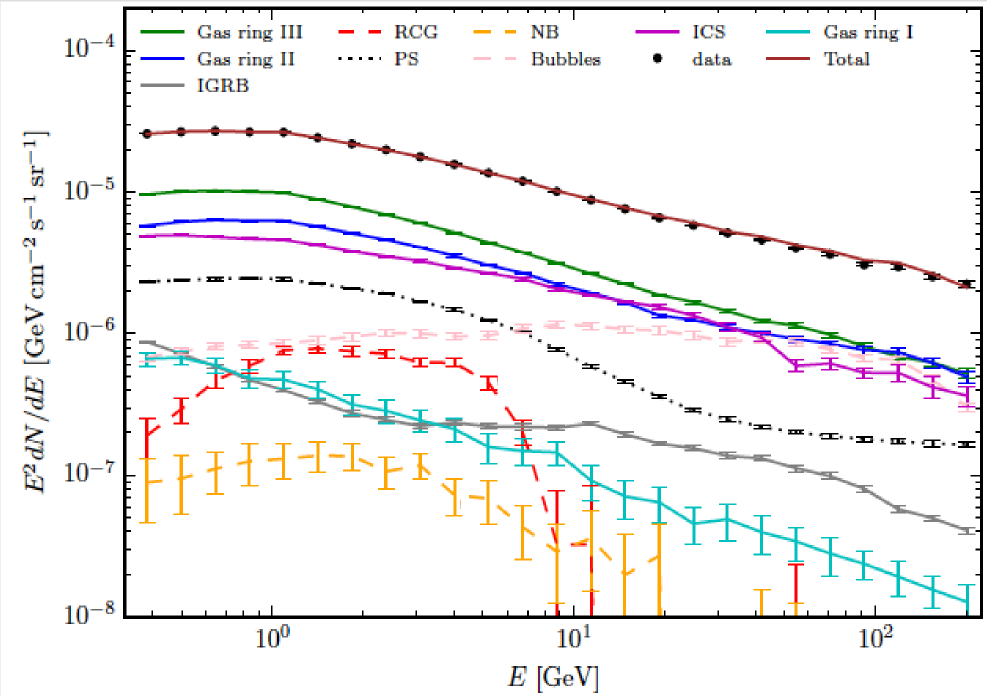

Fit in central 40x180 degrees, which facilitates the fitting of gas template rings (x3) and provides leverage to disentangle components.

Regularization by modulation parameters account for small-scale model inaccuracies.

Boxy bulge

Nuclear bulge

We demonstrated that the stellar bulge model provides a significantly better fit ($> 10\sigma$) to the data than the DM-emission related Einasto or contracted NFW profiles. Hence the GCE appears to simply trace stellar mass in the bulge, not the dark matter density squared (although the actual DM profile is sufficiently uncertain that this possibility cannot be entirely excluded). What

Bartels et. al. Nat. Astr. (2018)

The Photon Statistics of the GeV Excess

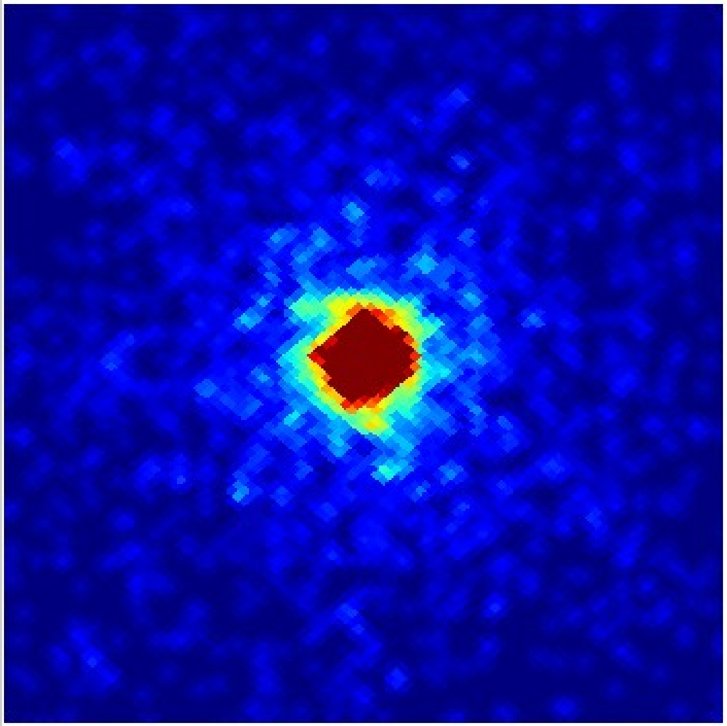

vs

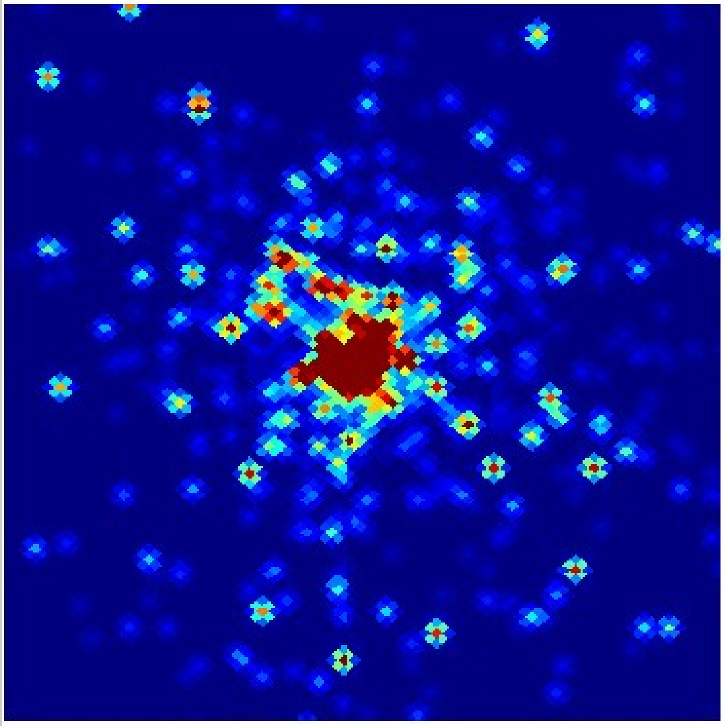

Lee et. al. PRL (2016)

Diffuse source vs point sources

The Photon Statistics of the GeV Excess

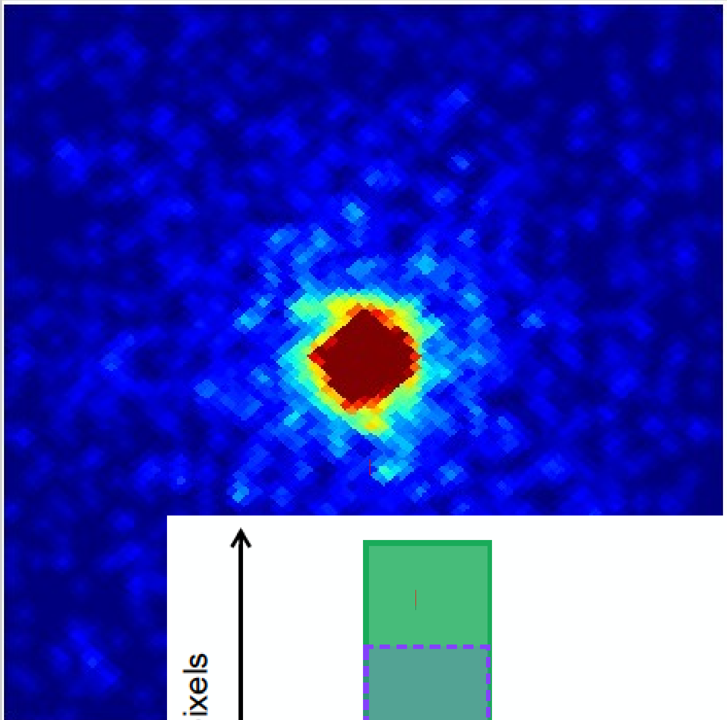

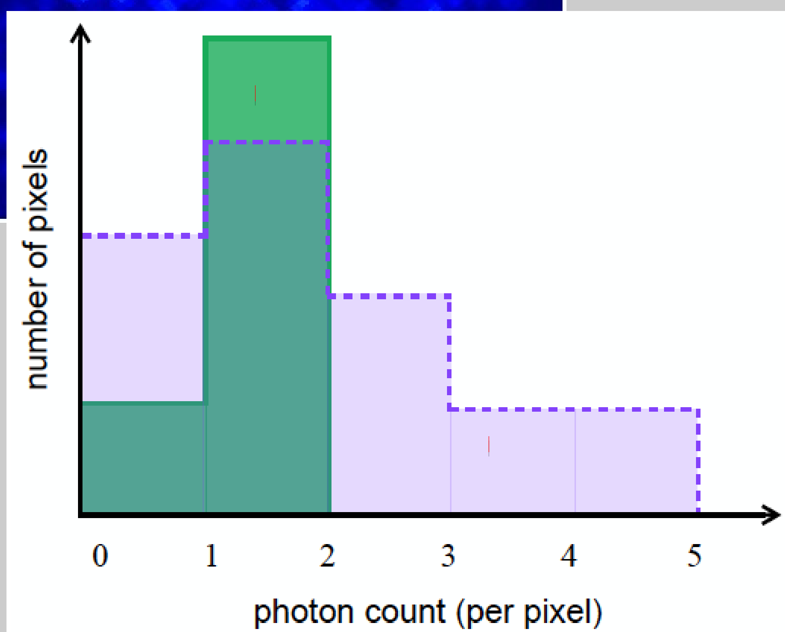

vs

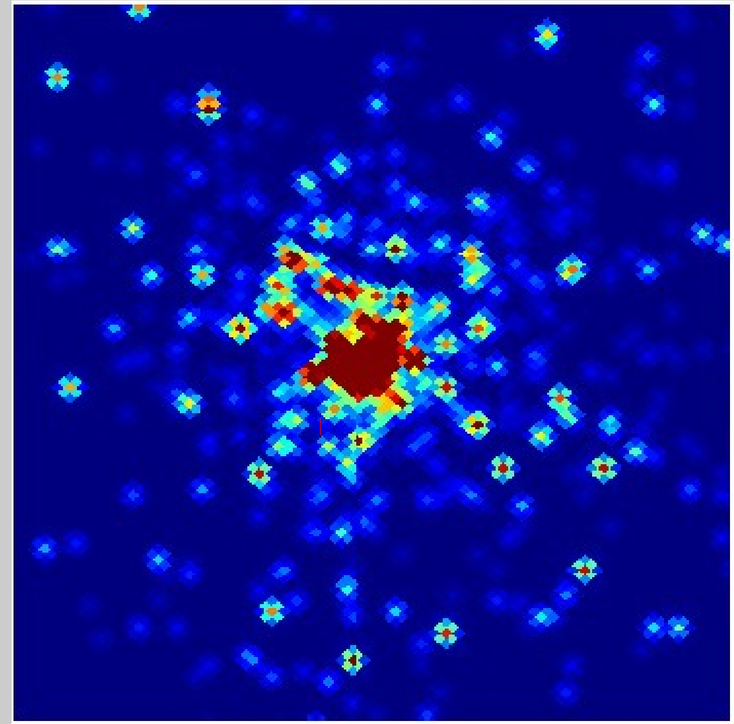

Lee et. al. PRL (2016)

Look for peaks on top of Poisson noise

Bartels et al (2016)

data

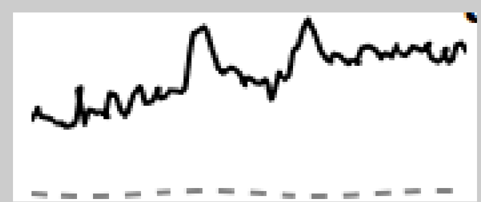

c.f. P(D) distribution in X-ray astronomy (Malyshev & Hogg 2011)

What have we learned so far?

1) Spectrum of the Galactic Center Excess?

Agrees well with spectrum of millisecond pulsars in Globular clusters

2) Spatial Morphology of the GCE?

Follows the distribution of stars in the Galactic bulge

3) Photon statistics?

Well described by non-Poissonian templates, which suggests an unresolved population of point sources in the GC.

How to detect the individual Millisecond Pulsars?

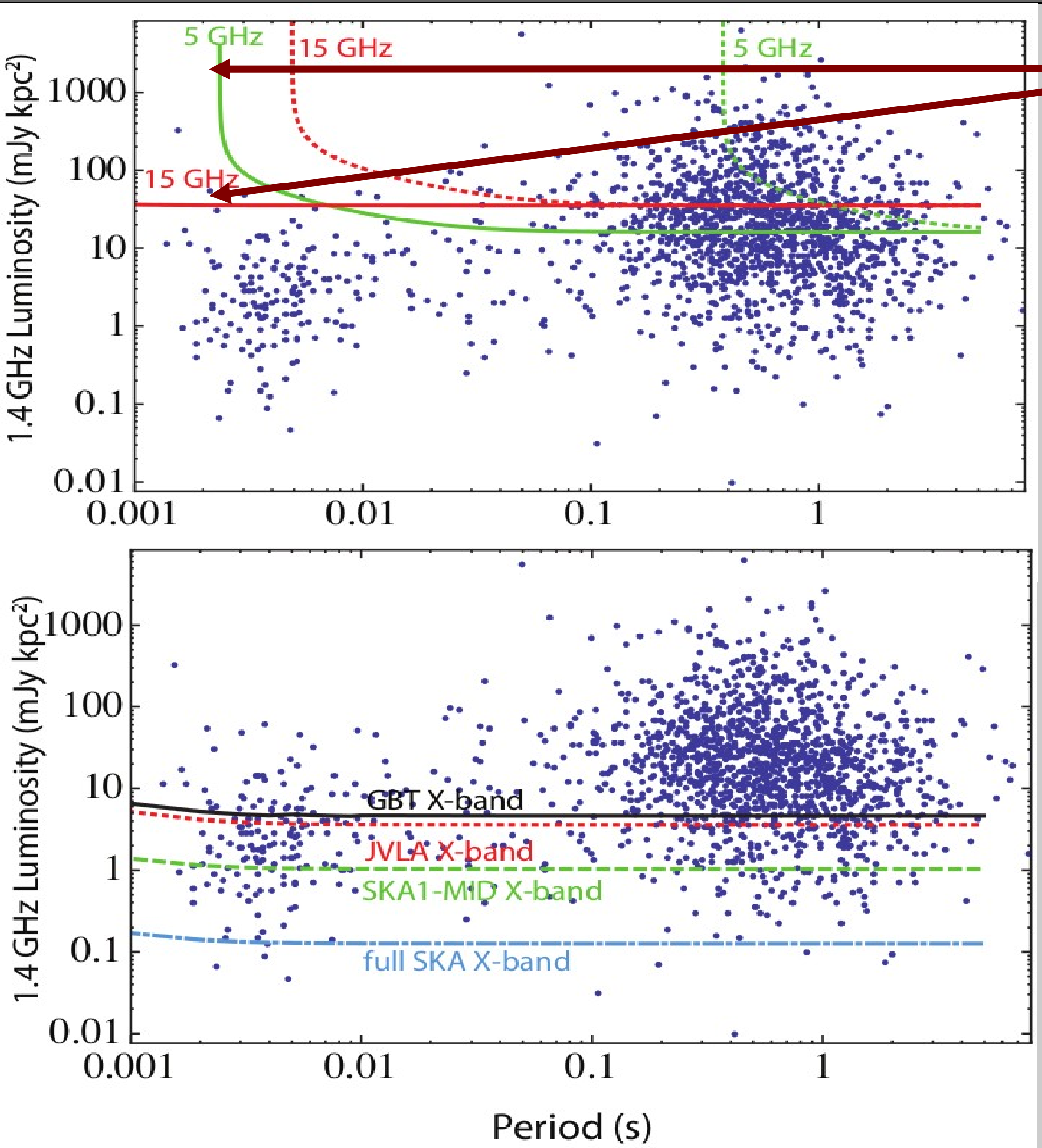

10σ sensitivities of previous 5 GHz and 15 GHz GBT searches at the GC

Deep X-band observations of GBT and VLA would be sensitive to a significant fraction of the known MSP population if located at the GC distance.

Macquart & Kanekar (2015)

CR electrons from MSPs could produce TeV gamma-ray signals

Song, OM, Horiuchi (in preparation)

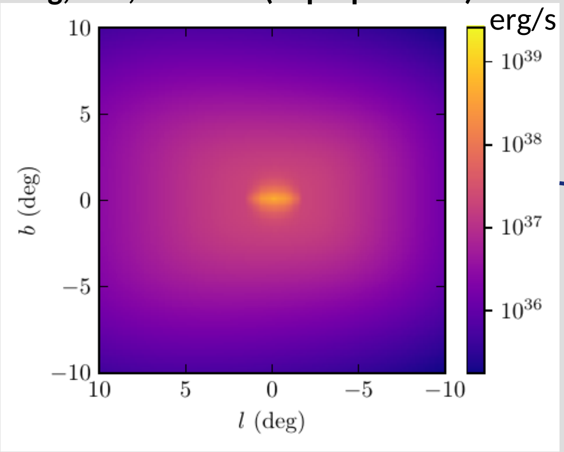

Cosmic Ray electron injection morphology

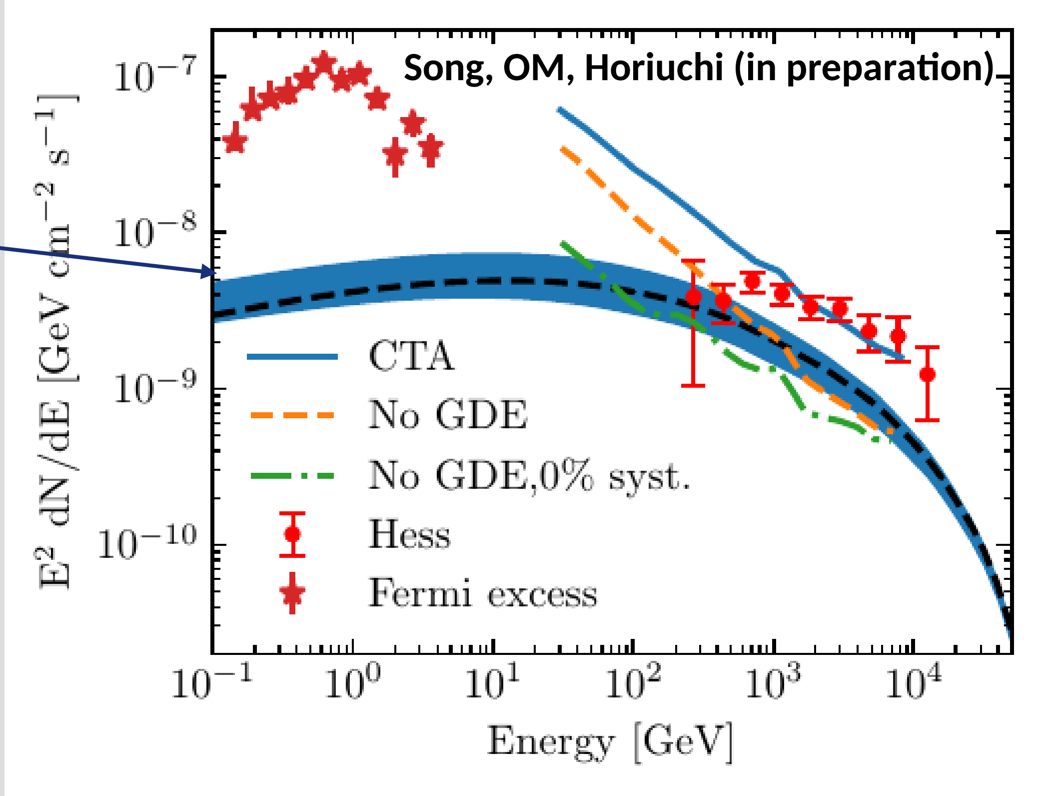

Inverse Compton spectrum of MSPs electrons.

Spatial morphology of MSPs Inverse Compton emission

Song, OM, Horiuchi (in preparation)

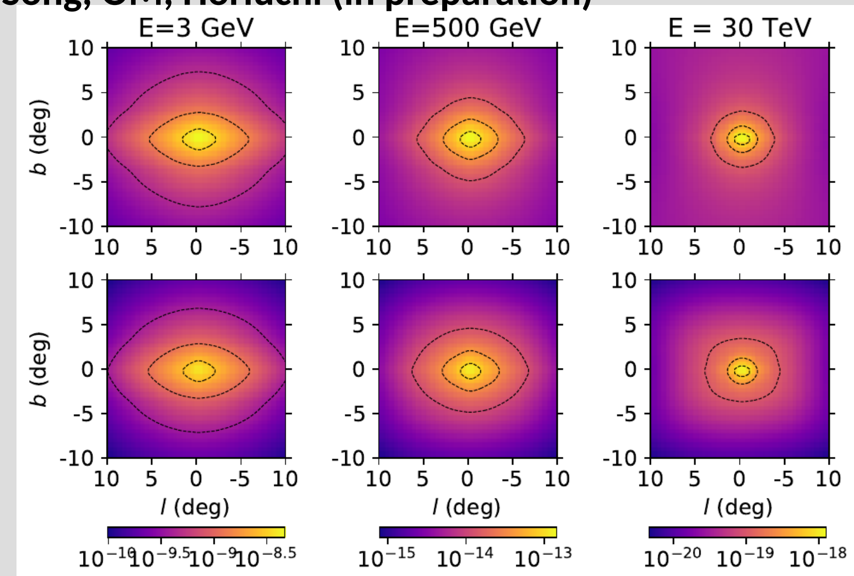

Inverse Compton from MSPs following spherical distribution

Inverse Compton from MSPs following a peanut bulge distribution

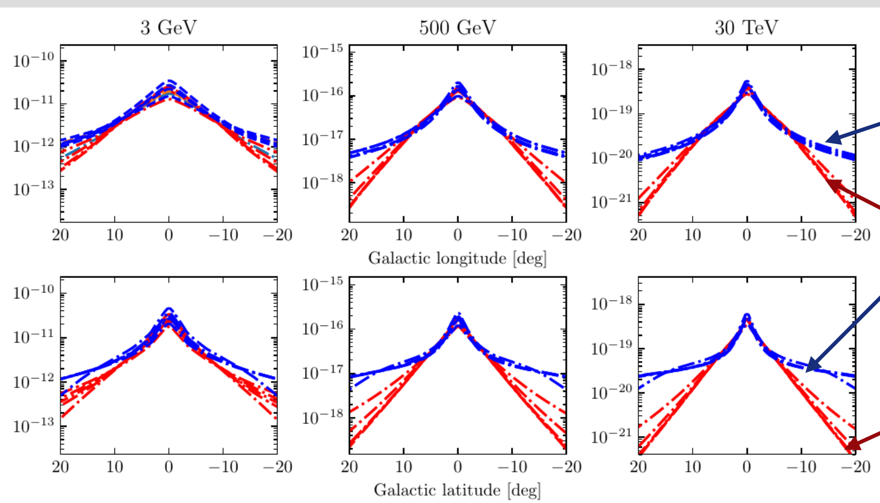

Spherical distribution

Peanut bulge distribution

The origin of the positrons producing the 511 keV emission

Knodlseder et al., 2005

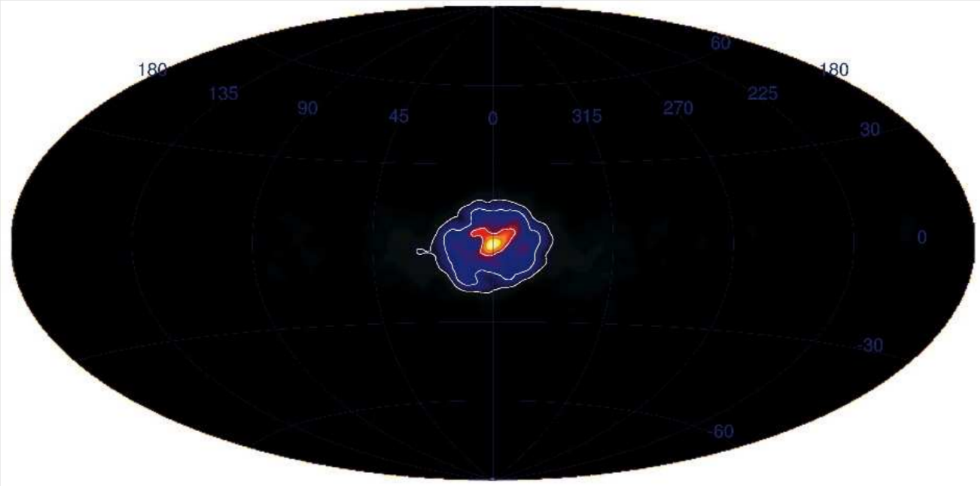

511 keV emission at the Galactic Center

1. Bulge/Disk<1 [Siegert+2016]

2. Injection of 2x10^42 positrons/s.

2. Guaranteed contribution from 26Al and 44Ti in core-collapse SN (~ 10% estimated).

3. Sgr A* [Totani 2006], pulsars [Wang+2006], Galactic X-ray binaries [Guessoum+2006], NS-NS merger [Fuller+2018] can supply additional positrons.

Crocker+2016 proposed an additional source of 44Ti from thermonuclear SN (SN1991bg-like). Their stellar evolution model also predicts a population of MSPs in the Bulge.

Is there a connection between the the GCE and the 511 keV line?

Knodlseder et al., 2005

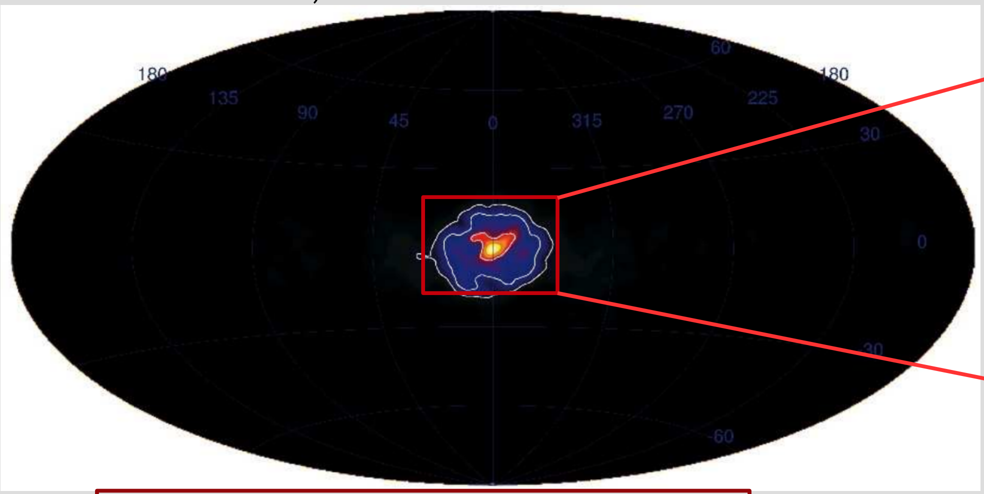

511 keV line morphology

Macias et al., 2018

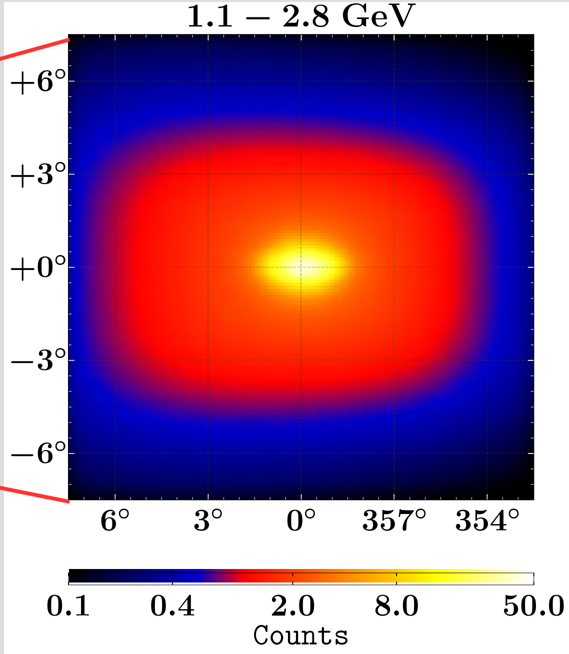

GCE morphology

There are remarkable similarities between the 511 keV line and the GCE

1. Stellar Bulge-like spatial morphology
2. Both extend ~10 degrees away from the Galactic Center
3. Both have a strong spectral peak close to Sgr A*

Conclusions

1) Dark matter emission in the Galactic Center?

→ Dark matter annihilation models **are excluded** by the data.

2) Gas Maps for the Galactic Center

→ **Hydrodynamical** gas maps provide a much improved fit to the data.

3) What is the Galactic Center excess due to?

→ Evidence is mounting for a **millisecond pulsar** population at the Galactic Center.

Thanks!

Back up slides

Detection Threshold

In our bin-by-bin analysis we had 19 energy bands in each of which the point source amplitude was not allowed to take on a negative value, we thus have a mixture distribution given by

$$p(\mathrm{TS}) = \frac{\delta(\mathrm{TS}) + \sum_{i=1}^{19} \binom{19}{i} \chi^2_{i+2}(\mathrm{TS})}{\sum_{i=0}^{19} \binom{19}{i}}$$

To work out the number of σ of a detection we evaluate the equivalent p-value for a one new parameter case:

$$\text{Number of } \sigma \equiv \sqrt{\mathrm{InverseCDF}\left(\chi^2_1, \mathrm{CDF}\left[\mathrm{p(TS)}, \hat{\mathrm{TS}}\right]\right)}$$

For 19 d.o.f a 4σ detection corresponds to TS>41.8.

Summary

- Analyzed Fermi-LAT Galactic center excess emission taking into account degeneracy with point sources and systematics in diffuse Galactic background.
- Interstellar gas maps constructed with the help of hydrodynamical simulations are a better description of the data than the ones constructed with the interpolation approach used in most previous works.
- Found 64 new gamma-ray point source candidates. Confirmed the existence of 31 new point sources in the 2FIG catalog.
- The spatial morphology is Galactic Center excess is spatially distributed as the previously known X-shaped bulge infrared emission and the nuclear bulge stellar population map.
- Found of order 10^4 or unresolved millisecond pulsars in the Xbulge could account for the excess emission.
- Annihilating dark matter is not longer a good fitting model for the Galactic center excess.

Additional Checks: Masking of the Galactic Plane

In preparation: Macias, Horiuchi et al.

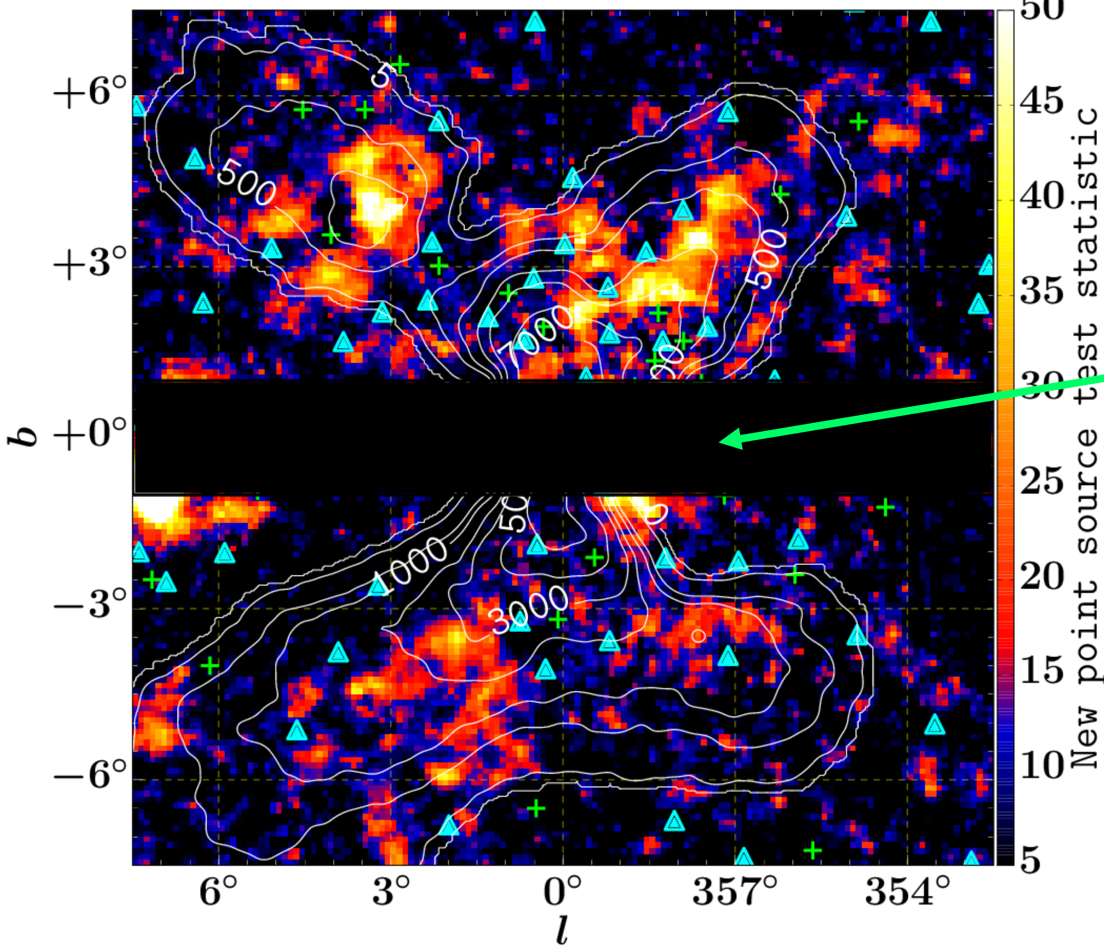

|b|< 1 degree masking of the Galactic plane

We have masked the Galactic plane (|b|<1 deg) and reran our maximum likelihood analysis.

Additional Checks: Masking of the Galactic Plane

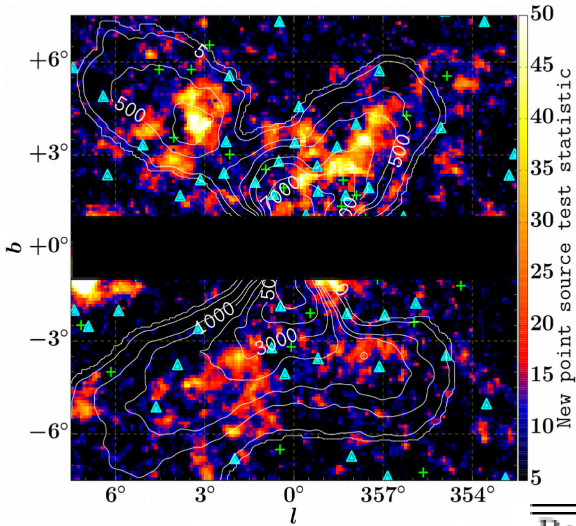

In preparation: Macias, Hoiuchi et al.

Base	Source	$\log(\mathcal{L}_{\rm Base})$	$\log(\mathcal{L}_{\rm Base+Source})$	$\mathrm{TS}_{\rm Source}$	σ	Number of source parameters
baseline	NFW	-430289.1	-430155.5	134	9.8	19
baseline	X-bulge	-430289.1	-430089.2	200	12.5	19
baseline	NP	-430289.1	-429657.8	631	12.9	22×19
baseline+NP	NFW	-429657.8	-429559.9	98	8.0	19
baseline+NP	X-bulge	-429657.8	-429496.6	322	16.5	19
baseline+NP+X-bulge	NFW	-429496.6	-429487.2	19	2	19

See the caption of Table I for definitions. After masking the Galactic plane ($|b| < 1°$), the number of new point sources (NP) added to the fit were 22.

When the Galactic plane is masked we still get that the X-shape bulge is preferred to an NFW source

Further Checks

Base	Source	$\log(\mathcal{L}_{\text{Base}})$	$\log(\mathcal{L}_{\text{Base+Source}})$	$\text{TS}_{\text{Source}}$	σ	Number of source parameters
baseline+NB+X-bulge	NFW	-171956.4	-171948.7	15	1.5	19
baseline+NFW	NB+X-bulge	-172167.9	-171948.7	438	18.6	2×19
baseline*	NFW	-173565.0	-172929.2	1272	34.6	19
baseline*+NFW	NB+X-bulge	-172929.2	-172592.0	674	23.8	2×19
baseline*+NB+X-bulge	NFW	-172631.5	-172592.0	79	6.9	19
baseline	2FIG	-172461.4	-170710.5	3501	37.3	81×19
baseline+2FIG	X-bulge	-170710.5	-170487.3	446	19.8	19
baseline+2FIG	NFW	-170710.5	-170484.6	452	19.9	19
baseline+2FIG	NB	-170710.5	-170470.5	480	20.6	19
baseline+2FIG+NB	NFW	-170470.5	-170387.8	165	11.1	19
baseline+2FIG+NB	X-bulge	-170470.5	-170307.6	326	16.6	19
baseline+2FIG+NB+Xbulge	NFW	-170307.6	-170301.8	12	1.1	19

To appear in a new version of Macias et al. (2016)

baseline:= Hydrodynamical gas maps
baseline*:= Interpolated gas maps
NP:= New point sources
NB:= Nuclear Bulge
FB:= Fermi Bubbles
2FIG:= 81 new point sources in the 15x15 RoI

Xco values at the Galactic Center

Ackermann et al. (2012)

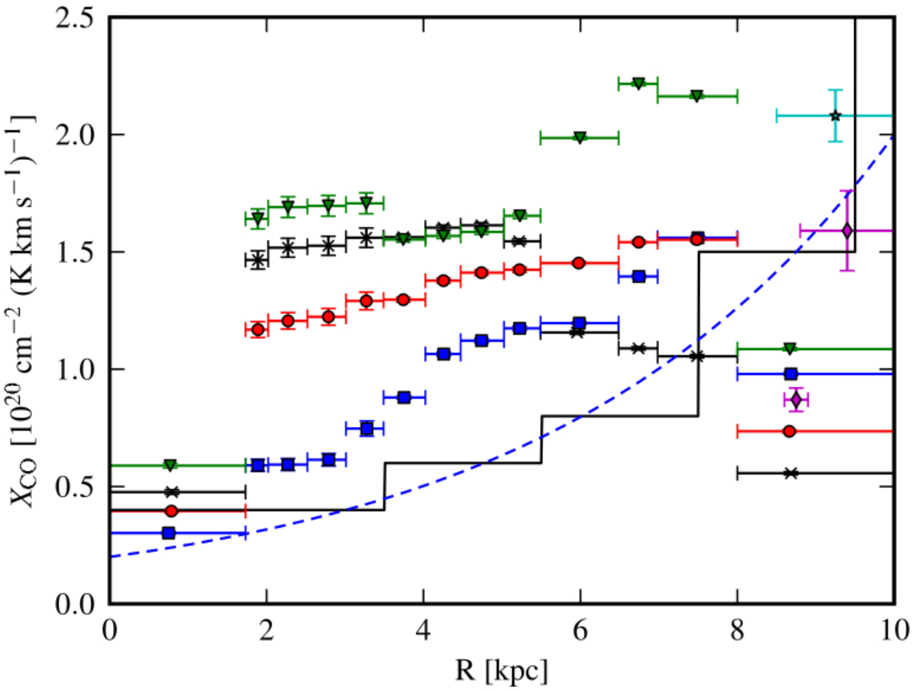

Radial distribution of Xco at the Galactic Center

Annulus	0 – 3.5 kpc	3.5 – 8.0 kpc	8.0 – 10.0 kpc
X_{CO}	0.4 ± 0.1	1.1 ± 0.2	3.6 ± 1.3

Macias et al. (2016)

Xco values are in agreement with those measured in the entire Galaxy.

Main arguments in the literature against an MSPs population at the Galactic Center

1) Paper I:

arXiv.org > astro-ph > arXiv:1512.04966

Astrophysics > High Energy Astrophysical Phenomena

The Gamma-Ray Luminosity Function of Millisecond Pulsars and Implications for the GeV Excess

Dan Hooper, Gopolang Mohlabeng

(Submitted on 15 Dec 2015)

2) Paper II:

arXiv.org > astro-ph > arXiv:1606.09250

Astrophysics > High Energy Astrophysical Phenomena

The Gamma-Ray Pulsar Population of Globular Clusters: Implications for the GeV Excess

Dan Hooper, Tim Linden

(Submitted on 29 Jun 2016 (v1), last revised 6 Jul 2016 (this version, v2))

3) Paper III:

arXiv.org > astro-ph > arXiv:1701.02726

Astrophysics > High Energy Astrophysical Phenomena

Low Mass X-Ray Binaries in the Inner Galaxy: Implications for Millisecond Pulsars and the GeV Excess

Daryl Haggard, Craig Heinke, Dan Hooper, Tim Linden

(Submitted on 10 Jan 2017)

Main arguments in the literature against an MSPs population at the Galactic Center

Argument I:

The luminosity distribution of the unresolved MSPs in the GC is inconsistent with the known resolved MSPs. In particular, Fermi should detect many more MSPs than currently Known.

Ploeg, Gordon, Crocker and Macias (2017)

Poegg, Gordon, Crocker, OM (2017)

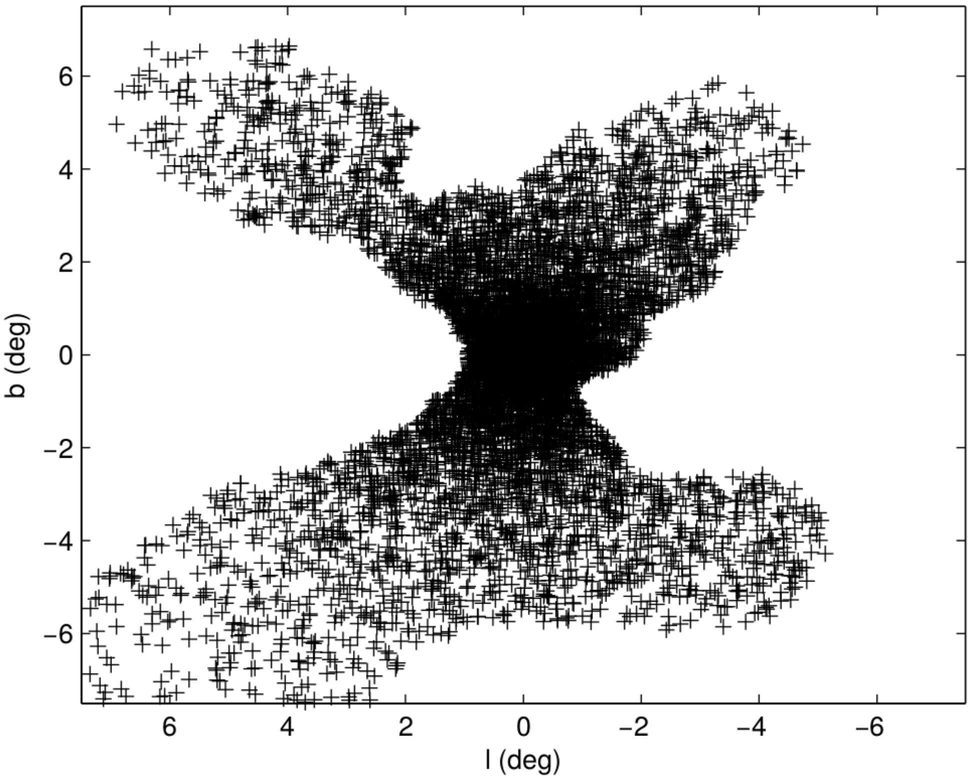

$$p(L) = \frac{1}{\sigma_L L\sqrt{2\pi}} \exp\left(\frac{-(\ln(L) - \ln(L_{\mathrm{med}}))^2}{2\sigma_L^2}\right)$$

$$\rho_{\mathrm{disk}}(r, z, N_{\mathrm{disk}}) = \frac{N_{\mathrm{disk}}}{4\pi\sigma_r^2\sigma_z} \exp(-r^2/2\sigma_r^2) \exp(-|z|/\sigma_z)$$

$$\rho_{\mathrm{bulge}}(r, N_{\mathrm{bulge}}) = \frac{3N_{\mathrm{bulge}}}{20\pi r_{\mathrm{bulge}}^{0.6}} r^{-2.4}, \quad 0 \le r < r_{\mathrm{bulge}}$$

$$p(F_{\mathrm{th}}) = \frac{1}{\sigma_{\mathrm{th}} F_{\mathrm{th}}\sqrt{2\pi}} \exp\left[\frac{-(\ln(F_{\mathrm{th}}) - (\mu_{\mathrm{th}}(l,b) + K_{\mathrm{th}}))^2}{2\sigma_{\mathrm{th}}^2}\right]$$

Performed MCMC simulations of disk and Bulge MSPs in the Galaxy.

Ploeg, Gordon, Crocker and Macias (2017)

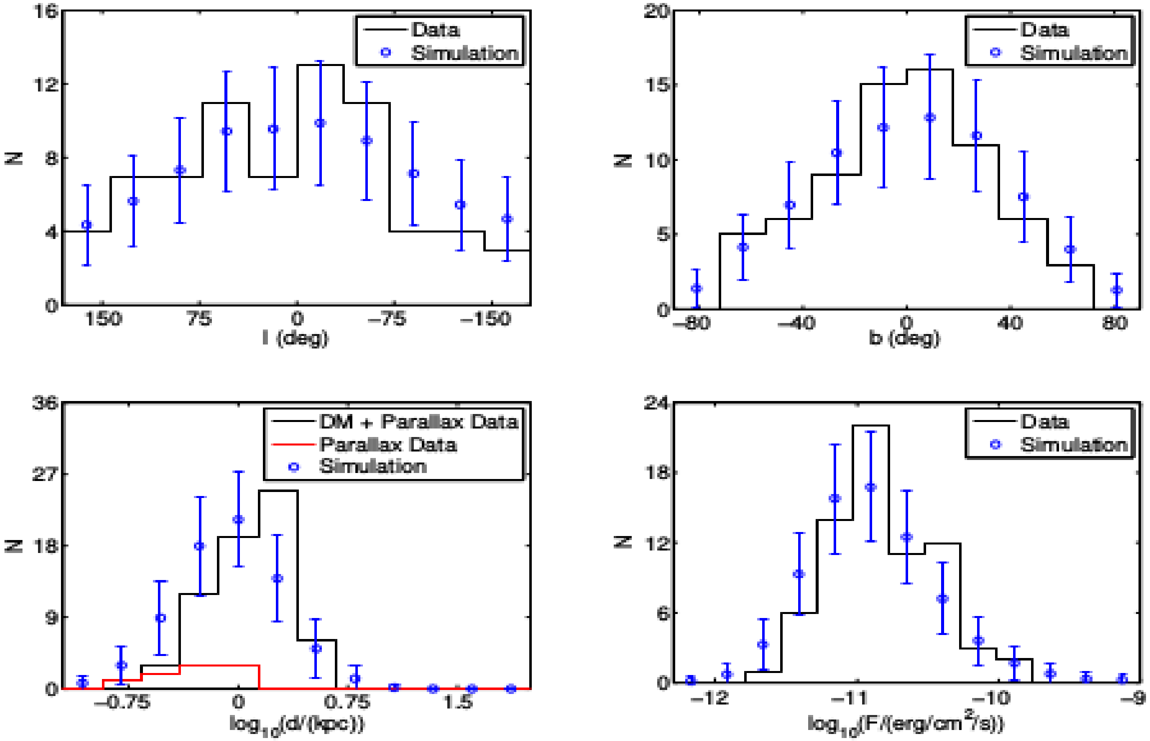

Poegg, Gordon, Crocker, OM (2017)

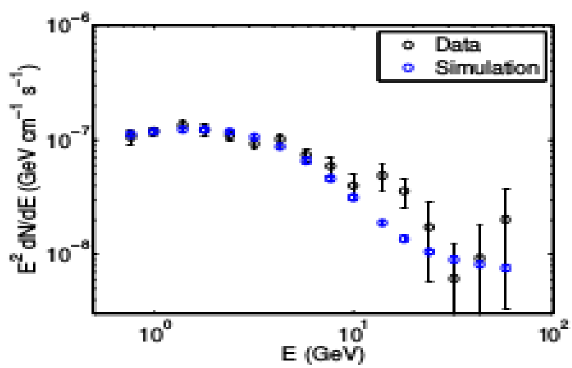

Parameter	Mean	Statistical Error
$\lambda_{\rm res}$	72	8
$\ln(r_{\rm d/b})$	1.6	0.3
$\log_{10}(L_{\rm med})$	31.8	0.5

Simulated MSPs explain GCE and do not overpredict resolved MSPs in the bulge or the disk.

Main arguments in the literature against an MSPs population at the Galactic Center

Argument II:

The number of LMXB and MSPs must be of similar magnitude, the same relative numbers of LMXB to MSPs should be seen in the GC and bulge as in other environments. However, the ratio of LMXBs to putative MSPs is much smaller for the GCE region than, for instance, globular cluster environments.

Main Arguments brought forward in those papers

Recycling MSPs Scenario

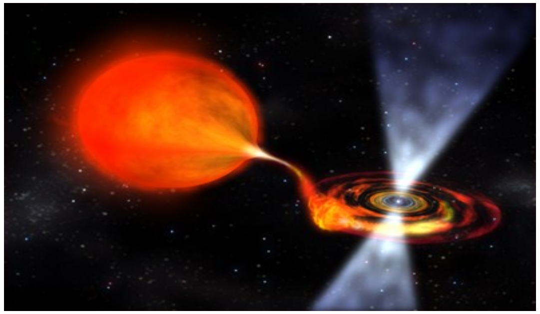

Image Credit: NASA/Dana Berry

Hooper et al. have implicitly assumed the *recycling MSPs* scenario!

At least two other MSPs formation channels exist that are not Disfavored by any data!

Accretion Induced collapse

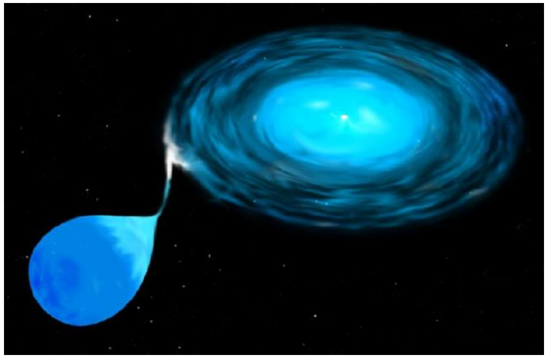

Image Credit: astrobits.org (?)

White dwarfs merger

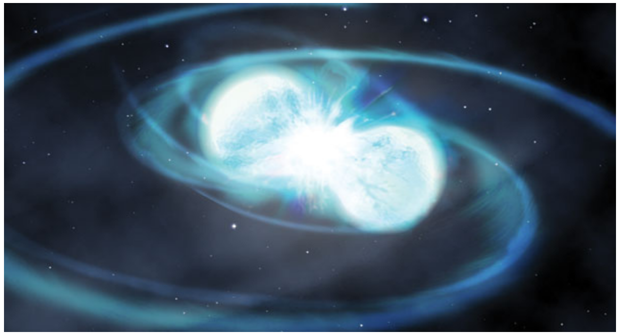

Image Credit: D. Andrew Howell
Nature 463, 35-36(7 January 2010).

Pulsar detection sensitivity (gamma-rays)

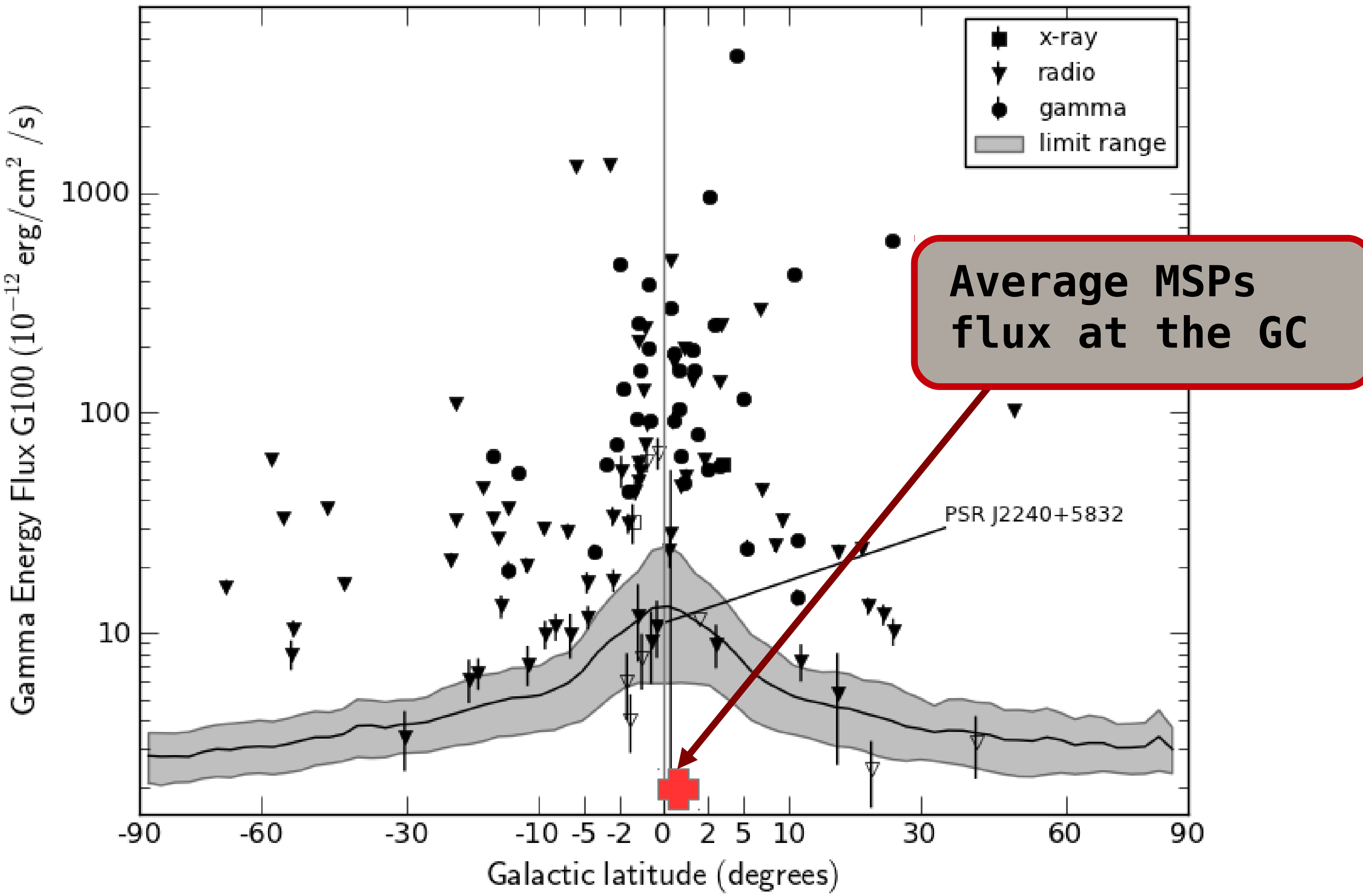

Credit: Fermi-LAT collaboration ApJ 208, 17 (2013)

Empirical maps accounting for observed residuals

Credit: Fermi-LAT collaboration ApJ.Suppl. 223 (2016) no.2, 26

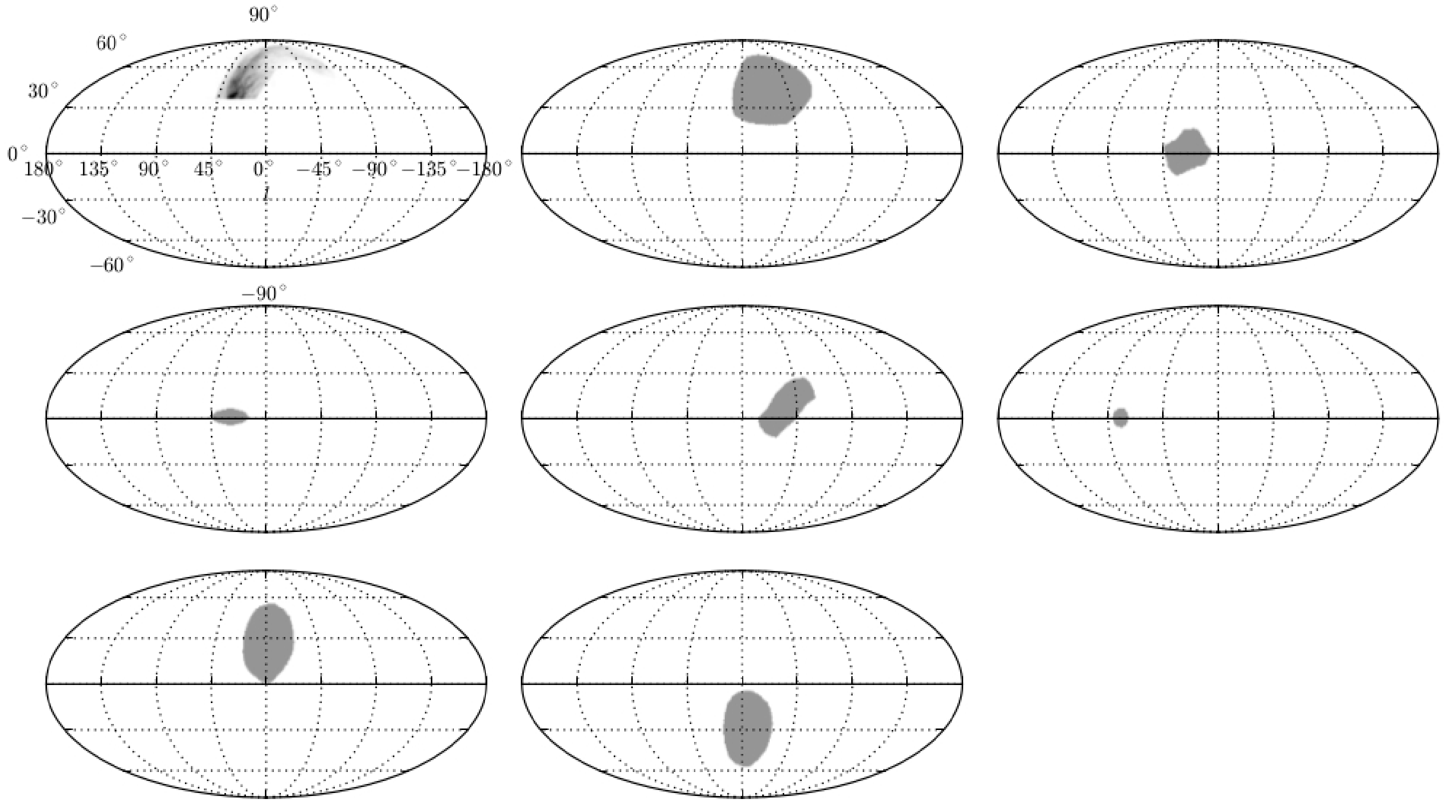

- The Fermi-LAT Galactic background model is only recommended for analyses of astrophysical compact objects.

Fermi Bubbles Vs X-shaped bulge

Ness & Lang (2016),
Macias et al. (2016)

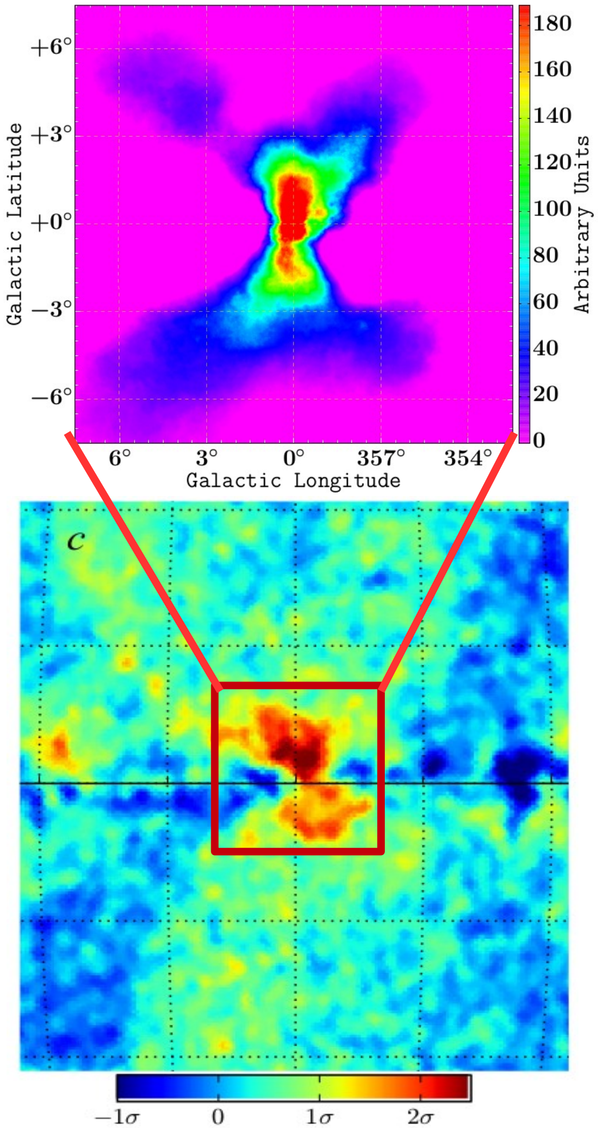

ApJ.Suppl. 223 (2016) no.2, 26

- **Recent work by the Fermi collaboration arguably shows a similar X-shaped excess at the base of the Fermi bubbles.**

- **However, our analysis shows distinct spectral characteristics to the overall Fermi bubbles ones: while the bubbles are described by $\propto E^{-1.9}$ the Xbulge is by $\propto E^{-2.34\pm0.05}$.**

- **The luminosity per solid angle of the X-bulge is $(2.7 \pm 0.3) \times 10^{38}$ erg/s/sr while that of the Fermi bubbles corresponds to $(6.3 \pm 0.1) \times 10^{37}$ erg/s/sr**

- **When our analysis considers the Fermi bubbles template proposed by ApJSup 223(2016)no.2,26 we find it has a negligible TS-value.**

Morphology of the Galactic Center excess in Ackermann et al. (2017)

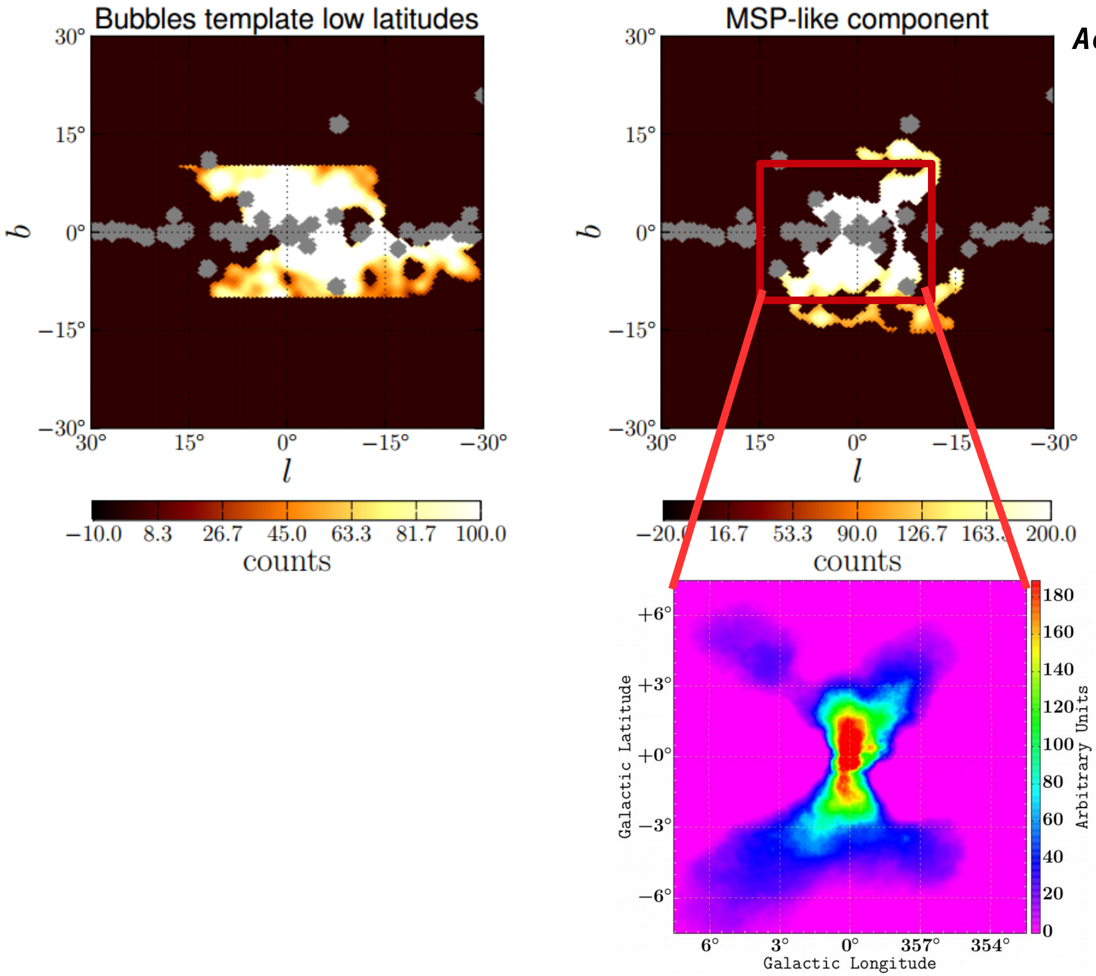

Ackermann et al. (2017)

Ness & Lang (2016), Macias et al. (2016)

MSPs-like component is concentrated in the inner 15x15 degrees and is not spherically symmetric

An unresolved population of Millisecond pulsars traced by the X-shaped and Nuclear Bulge could explain the Fermi GeV excess

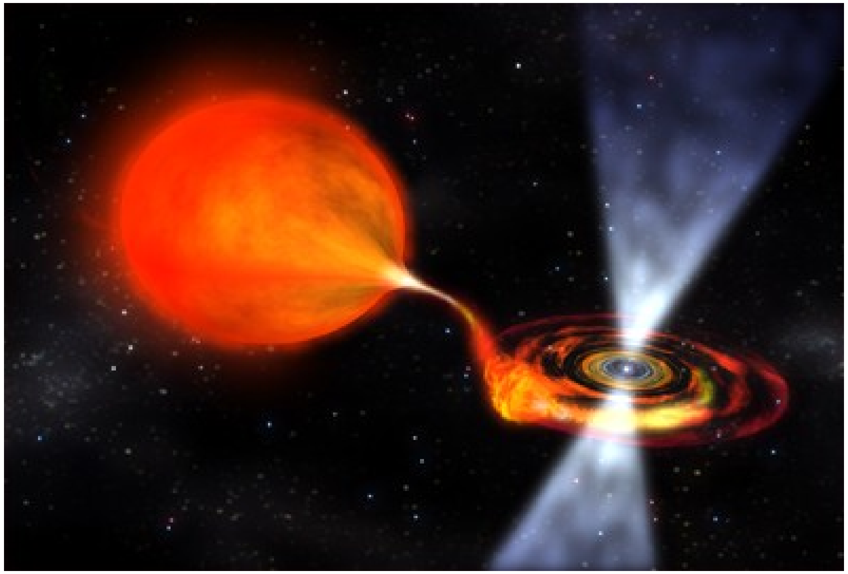

Image Credit: NASA/Dana Berry.

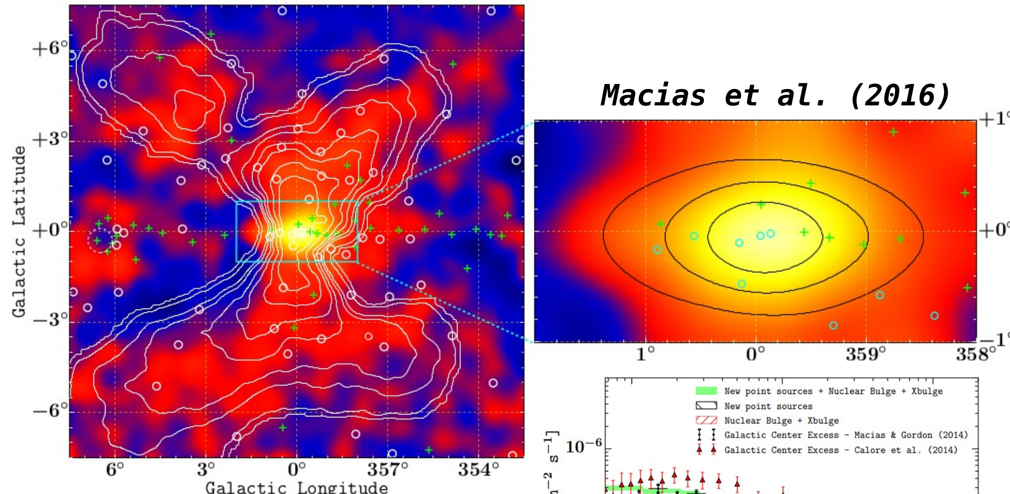

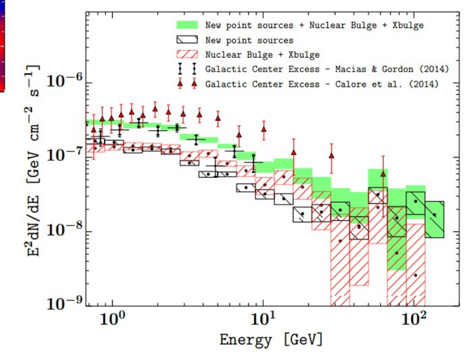

- **The stellar mass of the X-bulge plus the nuclear bulge is $\sim 2.9 \times 10^9\ M_\odot$ therefore the Luminosity-to-Mass ratio for E>100 MeV is $\sim 3 \times 10^{27}\ \mathrm{erg/s}/M_\odot$. From Winter et al. (2016) we infer the total MSPs luminosity of the Galaxy to be $\sim 2 \times 10^{27}\ \mathrm{erg/s}/M_\odot$ while for 47 Tuc is $\sim 5 \times 10^{28}\ \mathrm{erg/s}/M_\odot$.**

Observation − Simulation = “X” Leftovers

Using NASA's Wide-field Infrared Survey Explorer (**WISE**) ***Ness & Lang (2016)*** used these data to point out the X-shaped structure in the bulge of the Milky Way.

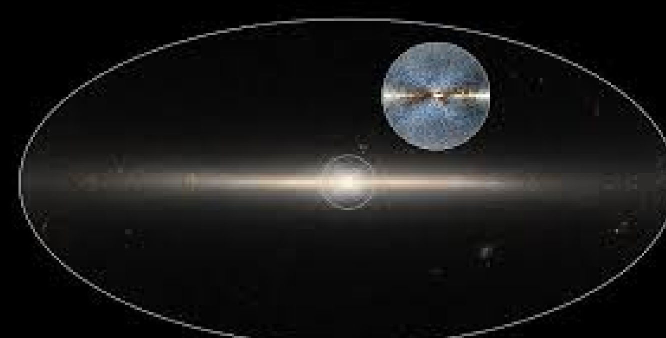

References

More details about this analysis can be found in

Evidence for gamma-ray emission from the X-shaped bulge of the Milky Way

By

OM, C. Gordon, R. Crocker, B. Coleman, D. Paterson, S. Horiuchi and M. Pohl

ArXiv:1611.06644

Main Results

Base	Source	$\log(\mathcal{L}_{\mathrm{Base}})$	$\log(\mathcal{L}_{\mathrm{Base+Source}})$	$\mathrm{TS}_{\mathrm{Source}}$	σ	Number of source parameters
baseline	FB	-172461.4	-172422.3	78	6.9	19
baseline	NFW-s	-172461.4	-172265.3	392	18.4	19
baseline	X-bulge	-172461.4	-172224.1	475	20.5	19
baseline	NFW	-172461.4	-172167.9	587	23.0	19
baseline	NB	-172461.4	-171991.8	939	29.5	19
baseline	NP	-172461.4	-169804.1	5315	55.7	64×19
baseline+NP	FB	-169804.1	-169773.6	61	5.8	19
baseline+NP	NB	-169804.1	-169697.2	214	13.0	19
baseline+NP	NFW	-169804.1	-169623.3	362	17.6	19
baseline+NP	X-bulge	-169804.1	-169616.2	376	18.0	19
baseline+NP+X-bulge	NFW	-169616.2	-169568.4	96	7.9	19
baseline+NP+X-bulge	NB	-169616.2	-169542.0	148	10.4	19
baseline+NP+X-bulge+NB	NFW	-169542.0	-169531.0	22	2.4	19
baseline+NP+X-bulge+NB	FB	-169542.0	-169525.5	33	3.5	19
baseline+NP+NB	X-bulge	-169697.2	-169542.0	310	16.1	19
baseline+NP+NFW	X-bulge+NB	-169623.3	-169531.0	185	10.8	2×19

To appear in a new version of Macias et al. (2016)

NP:=New point sources
NB:=Nuclear Bulge
FB:=Fermi Bubbles

baseline =

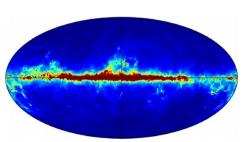

Gas rings

+

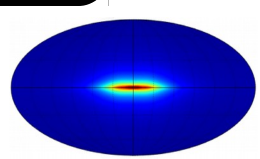

Inverse Compton

+

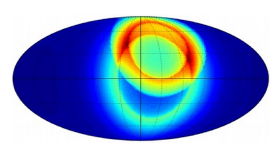

Loop I

+

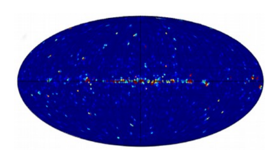

3FGL catalog

+

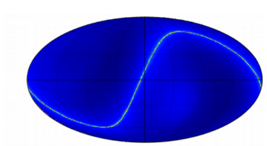

Sun&Moon

+ Isotropic model

Main Results

Base	Source	$\log(\mathcal{L}_{\text{Base}})$	$\log(\mathcal{L}_{\text{Base+Source}})$	$\text{TS}_{\text{Source}}$	σ	Number of source parameters
baseline	FB	-172461.4	-172422.3	78	6.9	19
baseline	NFW-s	-172461.4	-172265.3	392	18.4	19
baseline	X-bulge	-172461.4	-172224.1	475	20.5	19
baseline	NFW	-172461.4	-172167.9	587	23.0	19
baseline	NB	-172461.4	-171991.8	939	29.5	19
baseline	NP	-172461.4	-169804.1	5315	55.7	64×19
baseline+NP	FB	-169804.1	-169773.6	61	5.8	19
baseline+NP	NB	-169804.1	-169697.2	214	13.0	19
baseline+NP	NFW	-169804.1	-169623.3	362	17.6	19
baseline+NP	X-bulge	-169804.1	-169616.2	376	18.0	19
baseline+NP+X-bulge	NFW	-169616.2	-169568.4	96	7.9	19
baseline+NP+X-bulge	NB	-169616.2	-169542.0	148	10.4	19
baseline+NP+X-bulge+NB	NFW	-169542.0	-169531.0	22	2.4	19
baseline+NP+X-bulge+NB	FB	-169542.0	-169525.5	33	3.5	19
baseline+NP+NB	X-bulge	-169697.2	-169542.0	310	16.1	19
baseline+NP+NFW	X-bulge+NB	-169623.3	-169531.0	185	10.8	2×19

To appear in a new version of Macias et al. (2016)

NP:=New point sources
NB:=Nuclear Bulge
FB:=Fermi Bubbles

Main Results

Base	Source	$\log(\mathcal{L}_{\rm Base})$	$\log(\mathcal{L}_{\rm Base+Source})$	$\rm TS_{Source}$	σ	Number of source parameters
baseline	FB	-172461.4	-172422.3	78	6.9	19
baseline	NFW-s	-172461.4	-172265.3	392	18.4	19
baseline	X-bulge	-172461.4	-172224.1	475	20.5	19
baseline	NFW	-172461.4	-172167.9	587	23.0	19
baseline	NB	-172461.4	-171991.8	939	29.5	19
baseline	NP	-172461.4	-169804.1	5315	55.7	64×19
baseline+NP	FB	-169804.1	-169773.6	61	5.8	19
baseline+NP	NB	-169804.1	-169697.2	214	13.0	19
baseline+NP	NFW	-169804.1	-169623.3	362	17.6	19
baseline+NP	X-bulge	-169804.1	-169616.2	376	18.0	19
baseline+NP+X-bulge	NFW	-169616.2	-169568.4	96	7.9	19
baseline+NP+X-bulge	NB	-169616.2	-169542.0	148	10.4	19
baseline+NP+X-bulge+NB	NFW	-169542.0	-169531.0	22	2.4	19
baseline+NP+X-bulge+NB	FB	-169542.0	-169525.5	33	3.5	19
baseline+NP+NB	X-bulge	-169697.2	-169542.0	310	16.1	19
baseline+NP+NFW	X-bulge+NB	-169623.3	-169531.0	185	10.8	2×19

To appear in a new version of Macias et al. (2016)

NP:=New point sources
NB:=Nuclear Bulge
FB:=Fermi Bubbles

Main Results

Base	Source	$\log(\mathcal{L}_{\mathrm{Base}})$	$\log(\mathcal{L}_{\mathrm{Base+Source}})$	$\mathrm{TS}_{\mathrm{Source}}$	σ	Number of source parameters
baseline	FB	-172461.4	-172422.3	78	6.9	19
baseline	NFW-s	-172461.4	-172265.3	392	18.4	19
baseline	X-bulge	-172461.4	-172224.1	475	20.5	19
baseline	NFW	-172461.4	-172167.9	587	23.0	19
baseline	NB	-172461.4	-171991.8	939	29.5	19
baseline	NP	-172461.4	-169804.1	5315	55.7	64×19
baseline+NP	FB	-169804.1	-169773.6	61	5.8	19
baseline+NP	NB	-169804.1	-169697.2	214	13.0	19
baseline+NP	NFW	-169804.1	-169623.3	362	17.6	19
baseline+NP	X-bulge	-169804.1	-169616.2	376	18.0	19
baseline+NP+X-bulge	NFW	-169616.2	-169568.4	96	7.9	19
baseline+NP+X-bulge	NB	-169616.2	-169542.0	148	10.4	19
baseline+NP+X-bulge+NB	NFW	-169542.0	-169531.0	22	2.4	19
baseline+NP+X-bulge+NB	FB	-169542.0	-169525.5	33	3.5	19
baseline+NP+NB	X-bulge	-169697.2	-169542.0	310	16.1	19
baseline+NP+NFW	X-bulge+NB	-169623.3	-169531.0	185	10.8	2×19

To appear in a new version of Macias et al. (2016)

NP:=New point sources
NB:=Nuclear Bulge
FB:=Fermi Bubbles

Main Results

Base	Source	$\log(\mathcal{L}_{\mathrm{Base}})$	$\log(\mathcal{L}_{\mathrm{Base+Source}})$	$\mathrm{TS}_{\mathrm{Source}}$	σ	Number of source parameters
baseline	FB	-172461.4	-172422.3	78	6.9	19
baseline	NFW-s	-172461.4	-172265.3	392	18.4	19
baseline	X-bulge	-172461.4	-172224.1	475	20.5	19
baseline	NFW	-172461.4	-172167.9	587	23.0	19
baseline	NB	-172461.4	-171991.8	939	29.5	19
baseline	NP	-172461.4	-169804.1	5315	55.7	64×19
baseline+NP	FB	-169804.1	-169773.6	61	5.8	19
baseline+NP	NB	-169804.1	-169697.2	214	13.0	19
baseline+NP	NFW	-169804.1	-169623.3	362	17.6	19
baseline+NP	X-bulge	-169804.1	-169616.2	376	18.0	19
baseline+NP+X-bulge	NFW	-169616.2	-169568.4	96	7.9	19
baseline+NP+X-bulge	NB	-169616.2	-169542.0	148	10.4	19
baseline+NP+X-bulge+NB	NFW	-169542.0	-169531.0	22	2.4	19
baseline+NP+X-bulge+NB	FB	-169542.0	-169525.5	33	3.5	19
baseline+NP+NB	X-bulge	-169697.2	-169542.0	310	16.1	19
baseline+NP+NFW	X-bulge+NB	-169623.3	-169531.0	185	10.8	2×19

To appear in a new version of Macias et al. (2016)

NP:=New point sources
NB:=Nueclear Bulge
FB:=Fermi Bubbles

The Fermi GeV excess is best-fit by the X-bulge Nuclear Bulge. The NFW template does not improv the fit and is therefore not required by the da

Main Results: The Fermi GeV excess is correlated with X-shaped and nuclear bulge star populations!

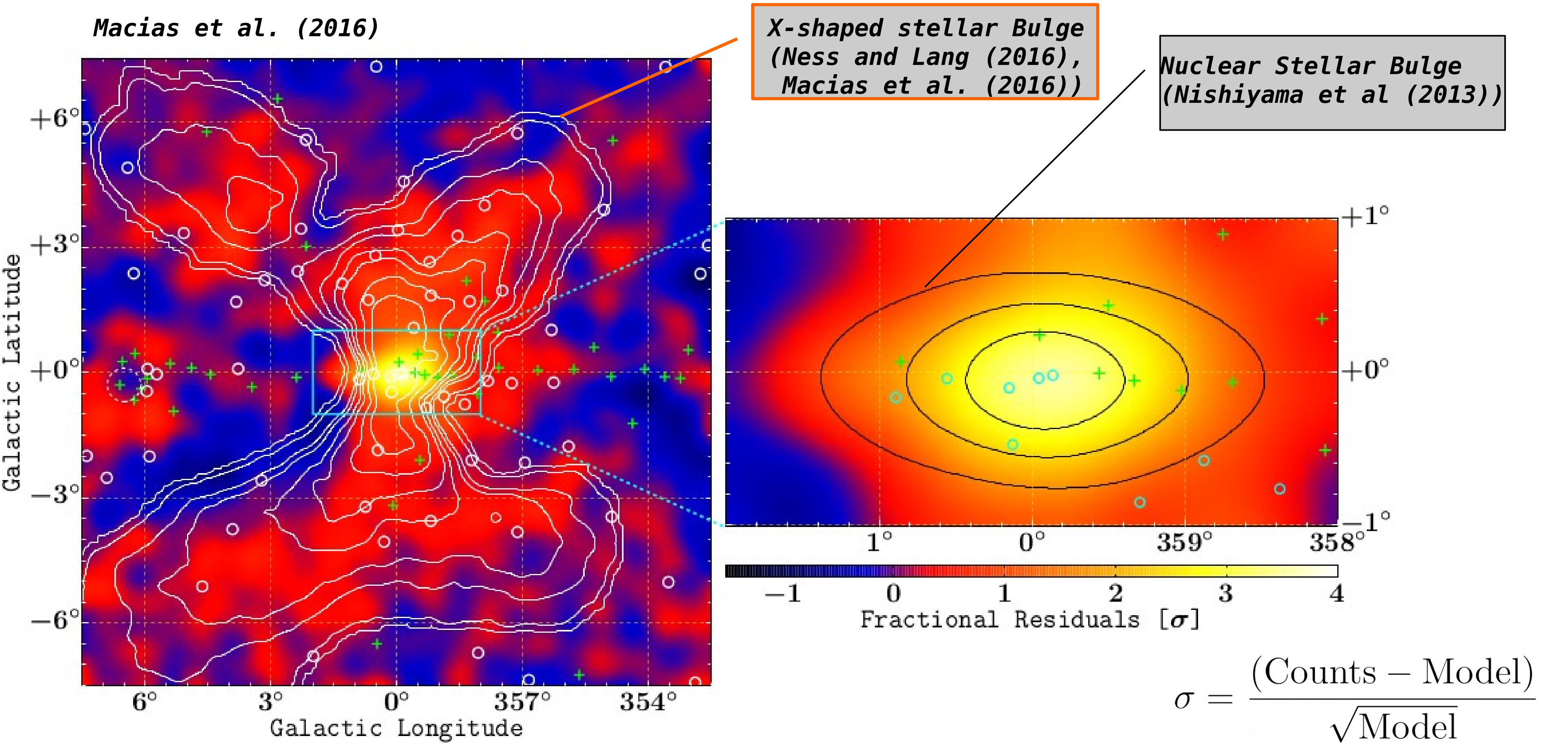

$$\sigma = \frac{(\mathrm{Counts} - \mathrm{Model})}{\sqrt{\mathrm{Model}}}$$

The Galactic Center excess gamma-rays are correlated with X-shaped and Nuclear bulge star

Multiwavelenght Observation of the GC

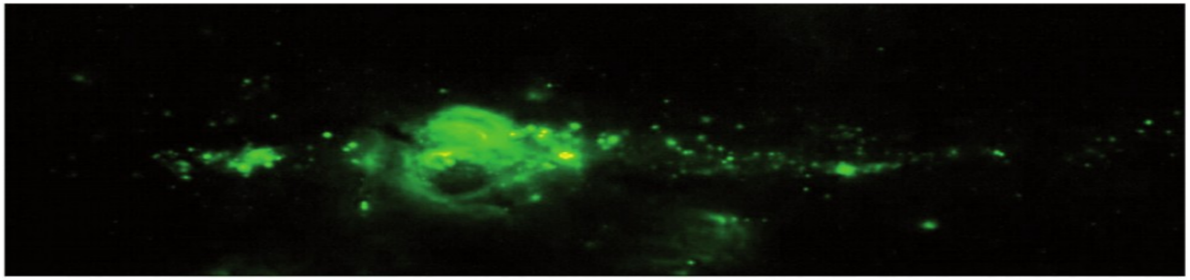

Infrared photons Credit: (Spitzer. Ramirez et.al 2007)

X-rays Credit: (Chandra, Muno, et.al 2008)

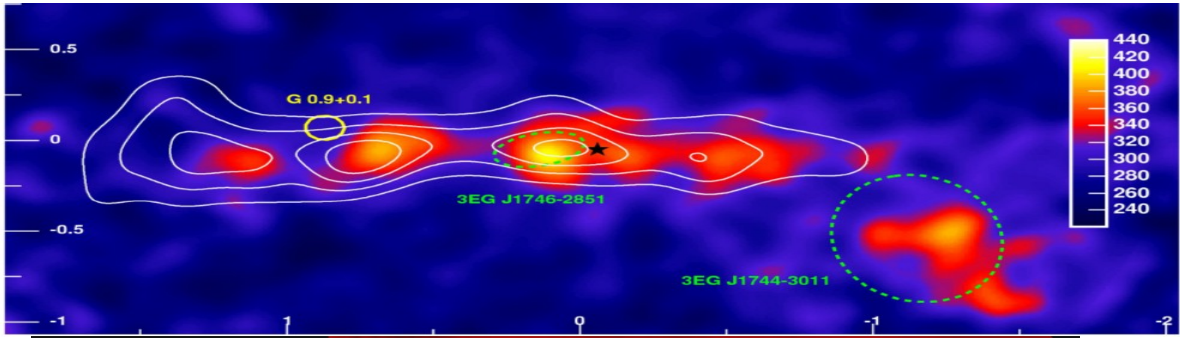

Diffuse ~TeV gamma-rays Credit: (H.E.S.S. Aharonian, et.al 2006)

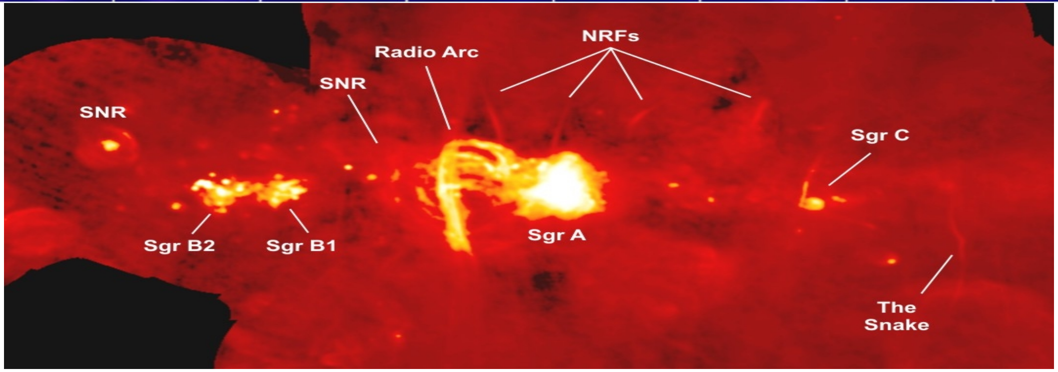

Combined radio image from the VLA (90 cm) and GBT. Credit: (NRAO/AUI/NSF Yusef-Zadeh, et.al)

Pulsar Emission Mechanism

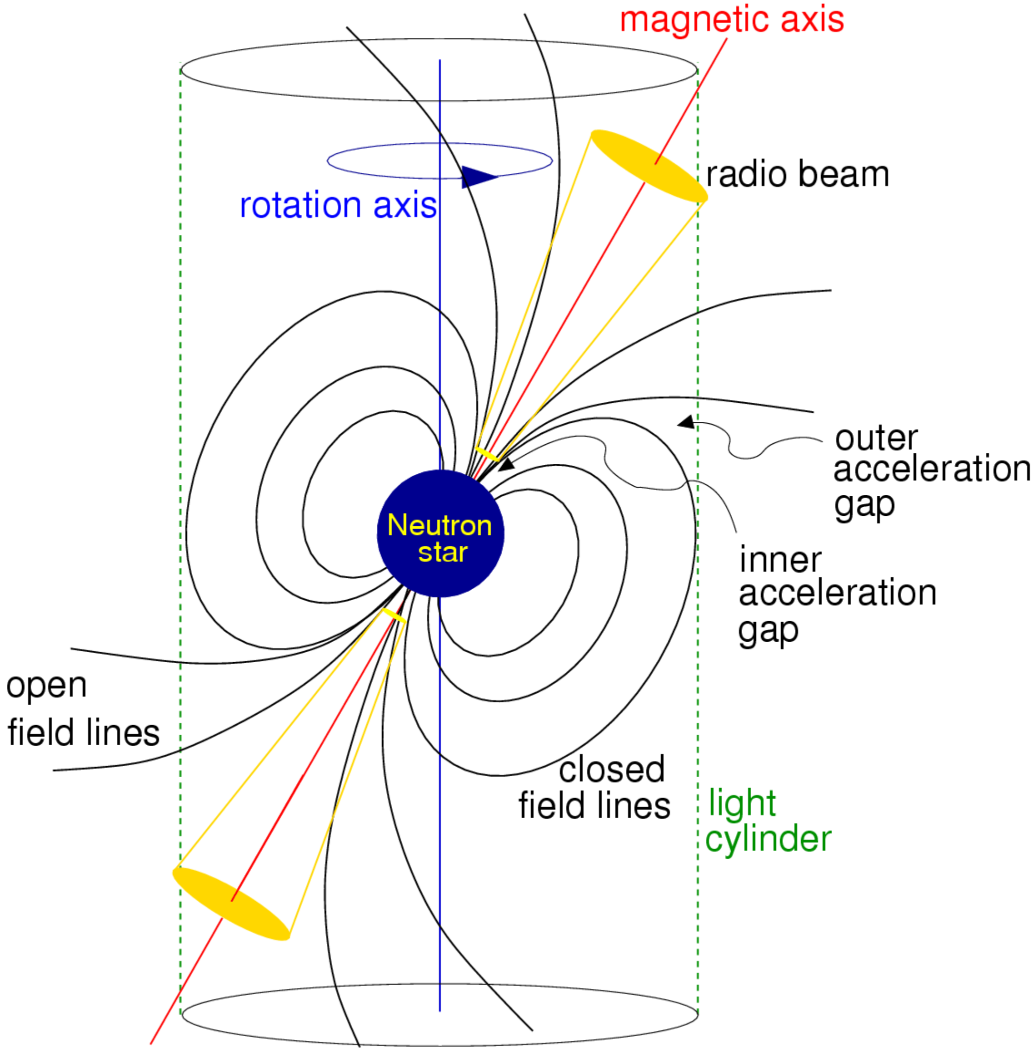

Image Credit: J. J. Condon and S. M. Ransom

Pulsar Emission Mechanism

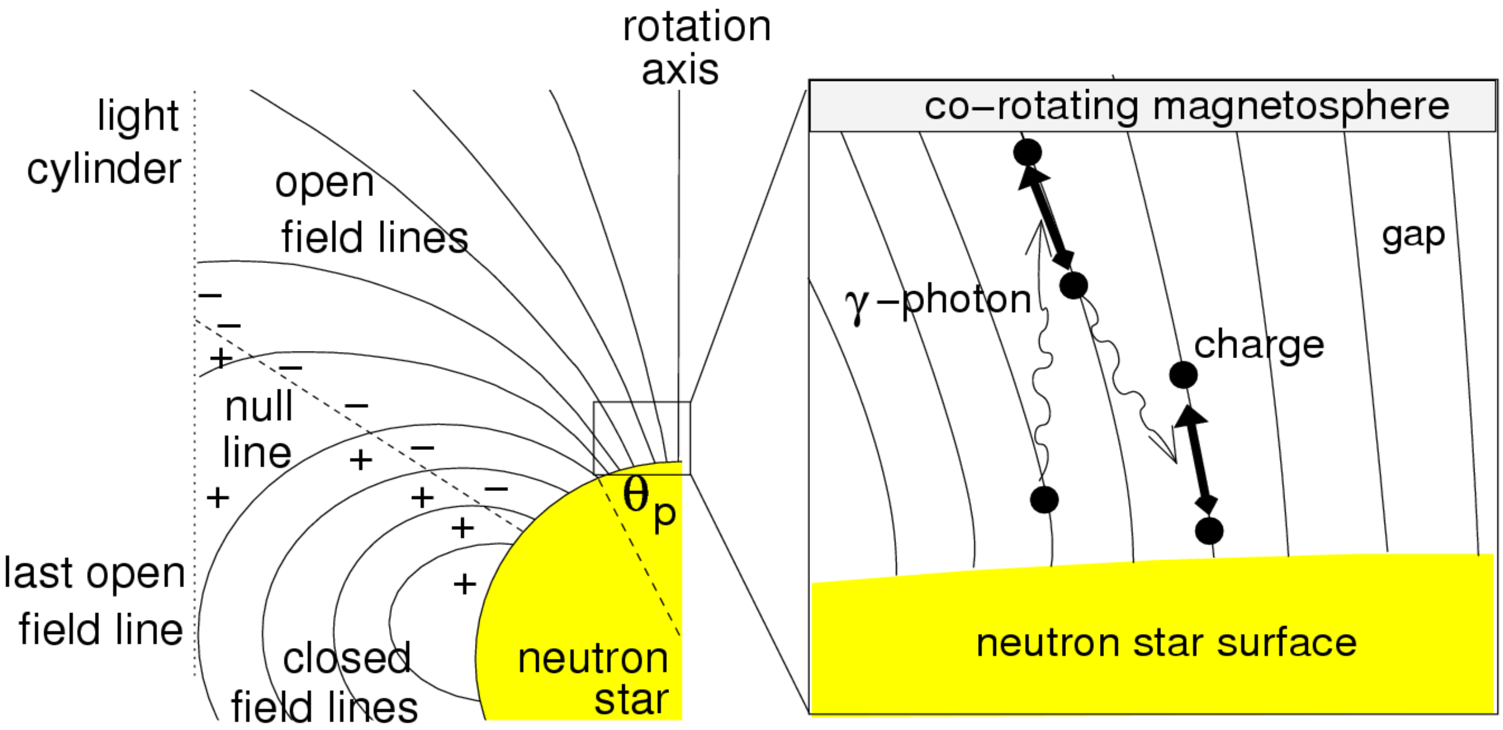

Image Credit: J. J. Condon and S. M. Ransom

The history of the Dark Matter puzzle

Henri Poincaré

"...since the velocity dispersion predicted in Kelvin's estimate is of the same order of magnitude as that observed, the amount of ***dark matter*** *was likely to be less than or similar to that of visible matter..."*

[Henri Poincaré (1906)]

Bertone & Hooper (2016) [ArXiv:1605.04909]

The term "Dark Matter" was likely first coined by Henri Poincaré in 1906.